Original Research Article

Targeting redox regulatory site of protein kinase B impedes neutrophilic inflammation

Po-Jen Chen[1,2], I-Ling Ko[1], Chia-Lin Lee[3,4], Hao-Chun Hu[5], Fang-Rong Chang[5], Yang-Chang Wu[5], Yann-Lii Leu[1,2], Chih-Ching Wu[6,7], Yung-Fong Tsai[1,8], Cheng-Yu Lin[1], Chang-Yu Pan[1], and Tsong-Long Hwang[1,2,8,9,*]

[1]Graduate Institute of Natural Products, College of Medicine, Chang Gung University, Taoyuan 333, Taiwan

[2]Chinese Herbal Medicine Research Team, Healthy Aging Research Center, Chang Gung University, Taoyuan 333, Taiwan

[3]Chinese Medicine Research and Development Center, China Medical University Hospital, Taichung 404, Taiwan

[4]Department of Cosmeceutics, China Medical University, Taichung 404, Taiwan

[5]Graduate Institute of Natural Products, College of Pharmacy and Research Center for Natural Products & Drug Development, Kaohsiung Medical University, Kaohsiung 807, Taiwan

[6]Department of Medical Biotechnology and Laboratory Science, College of Medicine, Chang Gung University, Taoyuan 333, Taiwan

[7]Department of Otolaryngology - Head & Neck Surgery, Chang Gung Memorial Hospital, Taoyuan 333, Taiwan

[8]Department of Anaesthesiology, Chang Gung Memorial Hospital, Taoyuan 333, Taiwan

[9]Research Center for Chinese Herbal Medicine, Research Center for Food and Cosmetic Safety, Graduate Institute of Health Industry Technology, College of Human Ecology, Chang Gung University of Science and Technology, Taoyuan 333, Taiwan

***Correspondence author:**

Dr. Tsong-Long Hwang, Ph.D.

Tel: +886 3 2118800 ext. 5523; Fax: +886 3 2118506; E-mail: htl@mail.cgu.edu.tw

Running title: Target Akt in neutrophilic inflammation

Keywords: Akt inhibitor; 5,7-dimethoxy-1,4-phenanthrenequinone; inflammation; neutrophils; lung injury

Abstract

Neutrophil activation has a pathogenic effect in inflammatory diseases. Protein kinase B (PKB)/Akt regulates diverse cellular responses. However, the significance of Akt in neutrophilic inflammation is still not well understood. Here, we identified 5,7-dimethoxy-1,4-phenanthrenequinone (CLLV-1) as a novel Akt inhibitor. CLLV-1 inhibited respiratory burst, degranulation, and chemotaxis in activated human neutrophils and neutrophil-like differentiated HL-60 (dHL-60) cells. CLLV-1 selectively inhibited Akt phosphorylation in activated human neutrophils and dHL-60 cells. Significantly, CLLV-1 blocked Akt kinase activity and covalently reacted with Akt Cys310 *in vitro*. The $Akt_{309\text{-}313}$ peptide-CLLV-1 adducts were determined by NMR or mass spectrometry assay. The level of alkylation agent-conjugated Akt (reduced form) was also inhibited by CLLV-1. Additionally, CLLV-1 ameliorated lipopolysaccharide-induced lung injury and complete Freund's adjuvant-caused inflammatory arthritis in mice. Together, CLLV-1 acts as covalent-allosteric Akt inhibitor via targeting Akt Cys310 to retrain inflammatory responses in human neutrophils and in inflammatory animals. Our findings provide a mechanistic framework for redox modification of Akt that may be a novel pharmacological target to alleviate neutrophilic inflammation.

Introduction

Neutrophils are the first line of host defense in innate immune response. Neutrophils are chemoattracted to inflammatory regions in response to infection, and they subsequently eliminate invading pathogens through respiratory burst, degranulation, and neutrophil extracellular traps (NETs). However, overwhelming activation of neutrophils plays a critical role both in infective and sterile inflammation (Jorch & Kubes, 2017; Leiding, 2017; Nauseef & Borregaard, 2014; Ortega-Gomez et al, 2013). The reactive oxygen species (ROS) and proteases released by activated neutrophils can damage healthy surrounding tissues, resulting in deleterious inflammatory diseases, such as acute respiratory distress syndrome (ARDS), chronic obstructive pulmonary disease (COPD), sepsis, or arthritis (Aschner et al, 2014; Delano & Ward, 2016; Jorch & Kubes, 2017; Soehnlein et al, 2017).

Pathogen recognition or an inflammatory environment triggers many critical intracellular signal processes through surface receptors in neutrophils (Lee et al, 2015; Liu et al, 2016; Tsai et al, 2016; Yang & Hwang, 2016). The serine/threonine-specific protein kinase, protein kinase B (PKB)/Akt, has been reported to regulate the immune responses of neutrophils, including respiratory burst, degranulation, and chemotaxis (Chamcheu et al, 2017; Kim et al, 2017; Manning & Toker, 2017; Zhang et al, 2013). In human neutrophils, activated Akt phosphorylates $p47^{phox}$, a component of nicotinamide adenosine dinucleotide phosphate (NADPH) oxidase, to initiate respiratory burst (Chen et al, 2010; Chen et al, 2003; El-Benna et al, 2009; Hoyal et al, 2003). Pharmacological inhibition of phospho-phosphoinositide 3-kinase (PI3K)/Akt signaling reduces the leukocyte degranulation (Hoenderdos et al, 2016; Nanamori et al, 2007). Akt also stabilizes F-actin polymerization to enhance the chemotaxis of activated neutrophils (Chen et al, 2010; Chodniewicz & Zhelev, 2003; Kumar et al, 2014). Therefore, Akt may be a potential pharmacological target to treat neutrophilic inflammation. Akt is activated via phosphorylation of Thr308 and Ser473 residues, and it is conversely turned off through dephosphorylation (Brazil et al, 2004; Weichhart et al, 2015). In addition to the well-known regulatory phosphorylation of Akt, emerging evidence has supported the significance of redox modification of Akt (Corcoran & Cotter, 2013; Zeng et al, 2018). Akt is inactivated through an intra-disulfide bond between Cys296 and Cys310 in the catalytic domain along with dephosphorylation (Ahmad et al, 2014; Durgadoss et al, 2012; Murata et al, 2003). However, the mechanistic details of whether redox-controlled Akt activity contributes to neutrophilic inflammation remains to be explored.

In this study, we identified that 5,7-dimethoxy-1,4-phenanthrenequinone (CLLV-1) (Fig 1A) is a novel Akt inhibitor via thiol-based reaction with the Cys310 residue of Akt to block the kinase activity. Phenanthrenequinones have been shown to exhibit antiplatelet aggregation and anticancer activity (Lee et al, 2012; Lee et al, 2014). Here, we found that CLLV-1 has an anti-inflammatory potential to impede respiratory burst, degranulation, and chemotaxis in activated human neutrophils or neutrophil-like differentiated HL-60 (dHL-60) cells. Moreover, administration of CLLV-1 and MK-2206 (an allosteric Akt inhibitor) attenuated the inflammatory responses of lipopolysaccharide (LPS)-induced acute lung injury (ALI) or complete Freund's adjuvant (CFA)-caused inflammatory arthritis *in vivo*. Our findings elucidate that redox modification of Akt may be a novel pharmacological target to suppress neutrophil-dominant disorders. We also suggest that CLLV-1 has potential to develop as an anti-inflammatory drug.

Results

CLLV-1 suppresses the inflammatory responses in fMLF-activated human neutrophils

To investigate the anti-inflammatory ability of CLLV-1, we first examined the effects of CLLV-1 on *N*-formyl-Met-Leu-Phe (fMLF)-induced respiratory burst, including superoxide anion production, ROS formation, and NADPH oxidase activation ($p47^{phox}$ phosphorylation) in human neutrophils. CLLV-1 dose-dependently inhibited the superoxide anion generation and ROS formation with IC_{50} values of 0.058 ± 0.006 and 0.106 ± 0.022 μM, respectively (Fig 1B and 1C). CLLV-1 did not induce LDH release, suggesting that CLLV-1 did not cause membrane damage and cytotoxicity (Appendix Fig S1A). We further evaluated how CLLV-1 inhibited the superoxide anion generation in fMLF-activated human neutrophils. In a cell-free xanthine/xanthine oxidase system, CLLV-1 (0.1-3 μM) did not exhibit a superoxide anion-scavenging ability (Appendix Fig S1B). Superoxide dismutase (SOD) was a positive control. Superoxide anion is produced by NADPH oxidase, a multicomponent enzyme complex, in human neutrophils (El-Benna et al, 2016; Hoyal et al, 2003). The isolated neutrophil membrane and cytosol fractions were used to examine the inhibitory effect of CLLV-1 on NADPH oxidase. CLLV-1 (0.3 and 3 μM) did not reduce superoxide anion production in sodium dodecyl sulfate (SDS)-reconstituted NADPH oxidase (Appendix Fig S1C). Diphenyleneiodonium (DPI; 10 μM), an NADPH oxidase inhibitor, was a positive control. The phosphorylation of $p47^{phox}$, a component of NADPH oxidase, was repressed by CLLV-1 in fMLF-activated human neutrophils (Fig 1D), suggesting that anti-inflammatory ability of CLLV-1 on respiratory burst may be through modulating upstream signaling of NADPH oxidase in human neutrophils.

Next, the effects of CLLV-1 on human neutrophil degranulation and chemotaxis were determined. CLLV-1 apparently repressed fMLF-induced elastase release with an IC_{50} value of 0.172 ± 0.011 μM (Fig 2A). In contrast, CLLV-1 failed to alter the activity of elastase in a cell-free assay (Appendix Fig S1D), suggesting that CLLV-1 inhibited human neutrophil degranulation also via the regulation of intracellular signaling pathway. In addition, integrin CD11b activation leads to neutrophils adhering to endothelial cells and subsequently induces neutrophil migration and infiltration. F-actin polymerization at the leading edge in polarized neutrophils governs the chemotaxis (Chodniewicz & Zhelev, 2003; Ley et al, 2007). CLLV-1 decreased the CD11b expression and the F-actin assembly in fMLF-activated human neutrophils. Furthermore, CLLV-1 suppressed the fMLF-induced neutrophils adhesion to bEnd.3 endothelial cells (ECs) and migration (Fig 2B-E and Appendix Fig S2).

CLLV-1 ameliorates the Akt activation in response to various stimuli in human neutrophils

A goal of this study is to identify the target protein of CLLV-1 in human neutrophils. The fMLF mainly binds to formyl peptide receptor 1 (FPR1) to activate neutrophils through multiple intracellular signaling pathways such as Akt and mitogen-activated protein kinases (MAPKs) (Dorward et al, 2015). CLLV-1 (0.1-3 μM) did not compete with the fluorescent-labeled fNLFNYK, an fMLF analog, for FPR1 binding (using fMLF as a positive control) (Appendix Fig S1E), ruling out the effect of CLLV-1 on FPR1. Therefore, the activations of Akt, ERK, JNK and p38 were examined in fMLF-activated human neutrophils. CLLV-1 inhibited the phosphorylation of Akt (Thr308 and Ser473) but not ERK, JNK, and p38 (Fig 3). Because CLLV-1 selectively restrained Akt activation, we wondered whether CLLV-1 suppressed Akt activation and inflammatory responses in different stimuli-activated human neutrophils, including sodium fluoride (NaF; direct G protein activator), WKYMVm (FPR2 agonist), interleukin-8 (IL-8), and leukotriene B4 (LTB_4) (Futosi et al, 2013; Zhang et al, 2013). CLLV-1 significantly inhibited NaF- and WKYMVm-induced superoxide anion generation in human neutrophils. Also, CLLV-1 showed inhibitory effects on elastase release in NaF-, WKYMVm-, IL-8-, and LTB_4-activated human neutrophils (Fig EV1). Notably, CLLV-1 significantly suppressed the phosphorylation of Akt (Thr308 and Ser473) in all stimuli-activated human neutrophils (Fig EV2), suggesting that Akt kinase may be the target of CLLV-1 in human neutrophils. Another potent Akt inhibitor, MK-2206 (Hirai et al, 2010), also inhibited the superoxide anion generation and elastase release in fMLF-activated human neutrophils (Fig EV3A-B), supporting that inhibition of Akt is a potential strategy to attenuate neutrophilic inflammation.

CLLV-1 inhibits the inflammatory responses and Akt activation in fMLF-activated dHL-60 cells

HL-60 cells were exposure to DMSO for 5 days to differentiate into neutrophil-like cells (dHL-60 cells). Usage of dHL-60 cells provided enough cells for several biochemical experiments instead of limited primary human neutrophils. The increased FPR1 expression and cellular morphology of dHL-60 were observed to represent the neutrophil-like status (Fig 4A and Appendix Fig S3). CLLV-1 diminished superoxide anion generation and intracellular ROS formation in fMLF-induced dHL-60 cells. CLLV-1 also repressed the $p47^{phox}$ phosphorylation and F-actin polymerization in fMLF-activated dHL-60 cells (Fig 4B-E and Appendix Fig S4A-B), suggesting that dHL-60 cells provide another inflammatory model and CLLV-1 still retrains the respiratory burst and chemotaxis in fMLF-activated dHL-60 cells. Importantly, CLLV-1

also attenuated fMLF-induced phosphorylation of Akt (Thr308 and Ser473) in dHL-60 (Fig 4F).

CLLV-1 directly alleviates Akt activity

We tested whether the CLLV-1-inhibited Akt phosphorylation is based on altering the activation of upstream kinases of Akt, including phospho-phosphoinositide-dependent protein kinase 1 (p-PDK1), phospho-mammalian target of rapamycin C2 (p-mTORC2), and p-PI3K (Brazil et al, 2004; Weichhart et al, 2015). CLLV-1 (0.3-3 μM) failed to affect the phosphorylation of PDK1 (S241), mTORC2 (S2481), and PI3K (Y199 of p85 subunit) in fMLF-activated dHL-60 cells and human neutrophils (Fig 5A and Appendix Fig S5). The level of PI3K-generated phosphatidylinositol-3,4,5-trisphosphate (PIP3) was also not changed by CLLV-1 in fMLF-activated dHL-60 cells (Fig 5B and Appendix Fig S4C). Protein kinase (PK)A has been shown to attenuate neutrophilic inflammation through inhibiting Akt activation (Sousa et al, 2010). However, CLLV-1 did not increase the level of cAMP. The PKA inhibitor, H89, did not reverse the CLLV-1-inhibited superoxide anion generation and elastase release in activated human neutrophils (Appendix Fig S6).

We suggest that CLLV-1 may directly target Akt *per se* to repress inflammation in human neutrophils. To explore this hypothesis, the nonradioactive Akt kinase assay was performed *in vitro*. Clearly, our data showed that CLLV-1 (0.3-3 μM) blocked the kinase activity of Akt *in vitro*. MK-2206 was used as a positive control to inhibit Akt activity (Fig 6 and EV3C).

CLLV-1 covalently reacts with the thiol group of Cys310 in Akt

To determine how CLLV-1 blocked the Akt kinase activity, the molecular docking of CLLV-1 with Akt was performed. Based on docking optimization (CDOCKER) and CHARMm force field, the CLLV-1-Akt binding modes were generated in receptor cavities with 10 poses. The binding of CLLV-1 and Akt with the most favorable energy was estimated with -CDOCKER (-474.532 kcal/mol). The *p*-benzoquinone, aromatic rings or carboxyl group of CLLV-1 were proposed to interact with R273, D274, L275, C310, G311, A317, L316, Y315, V320 or V330 residues of Akt (Fig 6A-B). Interestingly, Cys310 residue of Akt was predicted as a CLLV-1-binding site, and the redox modification of Cys310 in Akt is important for Akt enzymatic activity (Ahmad et al, 2014; Murata et al, 2003). Hence, CLLV-1 may bind to the thiol group of Cys310 to interfere with the Akt activity. To address this hypothesis, the reaction between CLLV-1 and synthetic Akt peptides, $Akt_{304-308}$ (ATMKT), $Akt_{309-313}$ (FCGTP), $Akt_{314-318}$ (EYLAP), and $Akt_{307-328}$ (KTFCGTPEYLAPEVLEDNDYGR), were determined by nuclear magnetic resonance (NMR) or mass spectrometry (MS) assay. CLLV-1 covalently

reacted with the $Akt_{309-313}$ to exhibit a new singlet peak at δ 7.00, but CLLV-1 did not react with adjacent $Akt_{304-308}$ and $Akt_{314-318}$ lacking cysteine residue in the ^{1}H NMR spectrum analysis (Fig 6C and EV4A). Furthermore, the Akt peptides-CLLV-1 adducts were also examined by MS (Fig 6D-E and EV4B). The molecular mass of $Akt_{309-313}$, $Akt_{307-328}$, and CLLV-1 were 524, 2389, and 268 Da, respectively. If CLLV-1 reacted with the Akt peptides, the proposed molecular mass of adducts would be 792 Da ($Akt_{309-313}$-CLLV-1) and 2657 Da ($Akt_{307-328}$-CLLV-1). The corresponding signals were observed by MS, including $Akt_{309-313}$ ($[M+H]^+$; 524.079), $Akt_{307-328}$ ($[M+H]^+$; 2389.124), $Akt_{309-313}$-CLLV-1 ($[M_{CLL}+H]^+$; 792.244) and $Akt_{307-328}$-CLLV-1 ($[M_{CLL}+H]^+$; 2655.102). In addition, the sodium adducts (plus 23 Da) were also found, $Akt_{309-313}$-Na ($[M+Na]^+$; 546.145), $Akt^{307-328}$-Na ($[M+Na]^+$; 2411.258) and $Akt_{309-313}$-CLLV-1-Na ($[M_{CLL}+Na]^+$; 812.264). Similarly, the results of MS confirmed that CLLV-1 did not react with the adjacent peptides, $Akt_{304-308}$ and $Akt_{314-318}$, which do not contain Cys310. These results suggested that CLLV-1 covalently reacted with the thiol group of Cys310 in Akt via an electrophilic addition.

To confirm the effect of CLLV-1 on Akt redox status in cells, we used the alkylation agent, 4-acetamido-4'-maleimidylstilbene-2,2'-disulfonic acid (AMS), to label reduced form of protein along with increasing molecular weight (Ahmad et al, 2014). The level of AMS-labeled Akt (reduced form) was increased in fMLF-activated dHL-60 cells. CLLV-1 (0.3-3 μM) dose-dependently decreased the AMS-labeled Akt levels in fMLF-activated dHL-60 cells (Fig 7A). It has been reported that oxidization of Cys310 residue in Akt diminished its enzymatic activity and increased the interaction between Akt and protein phosphatase 2A (PP2A) (Ahmad et al, 2014; Durgadoss et al, 2012; Murata et al, 2003). CLLV-1 induced the Akt-PP2A interaction in fMLF-activated dHL-60 cells (Fig 7B). These results suggest that CLLV-1 covalently targets Cys310 of Akt to alleviate the activity of Akt.

CLLV-1 attenuates the LPS-induced ALI and CFA-caused inflammatory arthritis in mice

To examine the anti-inflammatory potential of CLLV-1 *in vivo*, the effects of CLLV-1 on LPS-induced ALI and CFA-caused paw edema, two neutrophil-dominant inflammatory models, were tested in mice. Intratracheal instillation of LPS showed an increase in pulmonary myeloperoxidase (MPO), a neutrophil infiltration marker, which was inhibited by intraperitoneal injection of CLLV-1 (10 mg/kg) or MK-2206 (10 mg/kg) (Fig 8A). The total protein levels were measured to represent the severity of pulmonary edema. Both CLLV-1 and MK-2206 effectively attenuated LPS-induced increase of protein levels in lungs (Fig 8B). The histopathologic features of lungs showed that LPS triggered inflammatory cell infiltration, inter-alveolar septal

thickening, and interstitial edema. Moreover, LPS induced Ly6G (specific neutrophil marker)-positive infiltrated cells as well as Akt activation in the lungs. Noticeably, administration of CLLV-1 and MK-2206 ameliorated LPS-induced distortion of pulmonary architecture, Ly6G-positive infiltrated neutrophils, and Akt phosphorylation (Fig 8C), suggesting the therapeutic potential of CLLV-1 in neutrophil-dominant lung diseases. On the other hand, the intraplantar injection of CFA induced an increase in paw thickness in mice, which was also significantly reduced by CLLV-1 (10 mg/kg) and MK-2206 (10 mg/kg) (Fig EV5A). Moreover, CFA markedly elevated the expressions of Ly6G and MPO in the inflammatory paws and the treatment of CLLV-1 or MK-2206 abolished the CFA-induced neutrophil infiltration (Fig EV5B).

Together, CLLV-1 successfully impeded the inflammatory ALI and inflammatory arthritis *in vivo*, supporting that pharmacologically targeting redox modification of Akt is a potential strategy for treating neutrophilic inflammation.

Discussion

Neutrophils are the most abundant leukocytes and play a significant role in innate immunity. However, an enhanced ROS generation and protease release by activated neutrophils can cause cell and tissue damage (Nicolas-Avila et al, 2017; Soehnlein et al, 2017). Akt pathway is known to contribute in many neutrophil responses, including respiratory burst, degranulation, and chemotaxis; however, the regulatory mechanisms and significance of Akt in neutrophilic inflammation are still elusory (Chamcheu et al, 2017; Kim et al, 2017; Manning & Toker, 2017; Zhang et al, 2013). Here, we show that a synthetic phenanthrenequinone compound, CLLV-1, inhibits various stimuli-triggered inflammatory responses in human neutrophils or neutrophil-like dHL-60 cells. CLLV-1 selectively blocked Akt activity through covalently targeting Cys310 residue of Akt. Moreover, CLLV-1 attenuated the inflammatory responses in LPS-induced ALI and CFA-mediated inflammatory arthritis in mice, indicating that CLLV-1 is a potential anti-inflammatory compound and supports an example of disrupting the redox modulation of Akt to eliminate neutrophil-associated diseases.

Akt is composed of pleckstrin homology (PH) domain, catalytic kinase domain, and regulatory domain. With stimulation, Akt is activated and phosphorylated at Thr308 and Ser473 residues, leading to PH domain distant from the kinase domain. In contrast, the Akt kinase is dephosphorylated and inactivated by PP2A (Brazil et al, 2004; Weichhart et al, 2015). Till now, emerging evidence has supported the important role of redox modification of Akt in conformational dynamics (Corcoran & Cotter, 2013). An intramolecular disulfide bond between Cys296 and Cys310 in the catalytic domain of Akt is determined that prompts dephosphorylation via associating with PP2A. The oxidized and dephosphorylated Akt is considered to lose its kinase activity (Ahmad et al, 2014; Durgadoss et al, 2012; Murata et al, 2003). Cys-to-Ser mutation at 296 and 310 in Akt prevents the cadmium-inhibited Akt activity and cell survival in neuroblastoma cells (Ahmad et al, 2014), supporting the biological significance of the critical Cys in Akt. In the present study, we found that fMLF mitigated the oxidized Akt levels in dHL-60 cells, suggesting that reduced form of Akt belongs to active conformation. CLLV-1 apparently repressed the alkylation agent-labeled Akt levels (reduced form). Also, the Akt-PP2A interaction was increased by CLLV-1.

CLLV-1 was proposed to interact with Cys310 of Akt in molecular docking model (Fig 6A). The adduct of $Akt_{309\text{-}313}$ peptides and CLLV-1 exhibited a new singlet peak at δ 7.00 in the ^{1}H NMR spectrum (Fig 6C). The molecular mass of Akt peptides-CLLV-1 adducts (Akt peptide + CLLV-1 – 2 (two hydrogen) Da) were also detected in

MALDI-TOF MS, $Akt_{309-313}$-CLLV-1-Na ($[M_{CLL}+Na]^+$; 812.264) and $Akt_{307-328}$-CLLV-1 ($[M_{CLL}+H]^+$; 792.244) (Fig 6D-E), suggesting the reaction between Akt and CLLV-1 via an electrophilic addition. It has been reported that thiol-based association between electrophilic compounds and proteins possessed selectivity and specificity. The structural characteristic of proteins and stereo chemical structures of electrophiles specifically offered their targeting selectivity (Dennehy et al, 2006; Lame et al, 2003; Mi et al, 2011). The redox modulations of ERK, JNK or p38 have been characterized in response to intracellular ROS (Corcoran & Cotter, 2013). Low hydrogen peroxide (< 0.1 μM) induced the oxidation of Cys38 and Cys214 in ERK2 and increased phosphorylation of ERK2; in contrast, doxorubicin-induced oxidation of ERK2 was accompanied by dephosphorylation (Galli et al, 2008; Luanpitpong et al, 2012). Upon exposure to higher hydrogen peroxide (> 10 μM), cysteines of JNK2 (Cys41) and p38 (Cys162) were oxidized following activation and phosphorylation (Galli et al, 2008). We found that CLLV-1 repressed fMLF-induced Akt but not ERK, JNK, and p38 activation in human neutrophils (Fig 3), implying the specificity of CLLV-1.

Three isoforms of Akt have been identified, Akt1 (PKBα), Akt2 (PKBβ), and Akt3 (PKBγ), sharing 90% identity in kinase domain. Neutrophils contain only Akt1 and Akt2. Akt isoform-specific knockout mice has exhibited overlapping but distinct roles in activated neutrophils (Chen et al, 2010; Li et al, 2014). With fMLF stimulation, only Akt2 but not Akt1 translocated to the leading edge in polarized neutrophils and induced the superoxide anion generation and $p47^{phox}$ phosphorylation (Chen et al, 2010). In the present study, CLLV-1 significantly abrogated the Akt activation in response to various stimuli in human neutrophils (Fig 3 and EV2) and the CLLV-1-targeted Cys310 of Akt was identical among Akt1/2/3 (Fig 6), suggesting that CLLV-1 covalently react with both Akt1 and Akt2 in neutrophils. It has been reported that Akt controls $p47^{phox}$ phosphorylation and F-actin polymerization to trigger respiratory burst and chemotaxis in neutrophils, respectively (Chen et al, 2010; El-Benna et al, 2009; Kumar et al, 2014). CLLV-1 dose-dependently restricted the Akt-mediated $p47^{phox}$ phosphorylation and F-actin levels in fMLF-activated human neutrophils and dHL-60 cells (Fig 1, 2 and 4), confirming that CLLV-1-inhibited Akt activity is critical for following inflammatory activation in human neutrophils.

The developing Akt inhibitors are usually classified as ATP-competitive inhibitors and allosteric inhibitors (Keane et al, 2014; Nitulescu et al, 2016). ATP-competitive inhibitors such as GSK690693 (Heerding et al, 2008) significantly suppress Akt activity; however, the off-target effect is still of concern because of the highly conserved ATP binding site among AGC kinase family such as PKA and PKC (Jacinto & Lorberg, 2008). More and more allosteric inhibitors have been developed with higher efficacy and specificity such as MK-2206, an allosteric inhibitor of Akt (Hirai et

al, 2010). The Cys296 and Cys310 residues in Akt catalytic domain were identified as allosteric sites for regulating Akt activity (Lee et al, 2010; Nitulescu et al, 2016; Shearn et al, 2012). Therefore, the Cys296 and Cys310 residues of Akt are potential therapeutic targets in Akt-associated disorders. In this study, CLLV-1 was found to be a novel allosteric inhibitor of Akt through covalently binding to Cys310 *in vitro* (Fig 5B and 6). This is the first example to retrain neutrophilic inflammation via pharmacologically targeting redox regulatory site of Akt. CLLV-1 and MK-2206 showed anti-inflammatory effects in human neutrophils and ameliorated LPS-primed ALI and CFA-induced paw inflammation in mice (Fig 8 and EV5), supporting the therapeutic potential of CLLV-1 in neutrophilic lung damage and arthritis. Accordingly, the targeting redox modification of Akt would be a potential strategy to develop anti-inflammatory drugs.

In summary, we demonstrate that Akt activation plays a critical role in neutrophilic inflammation. Targeting Akt Cys310 using drug can regulate Akt phosphorylation and activity. Our findings also reveal an important example of how a novel derivative of phenanthrenequinone, CLLV-1, restrains neutrophil-associated inflammatory responses via inhibiting Akt activity in a redox-dependent manner (Fig 9).

Materials and Methods

Reagents

CLLV-1 was synthesized by our group (Lee et al, 2008). The structure of CLLV-1 was determined by ^{1}H NMR spectrum analysis (Fig 6C). The purity of CLLV-1 was higher than 96% as determined by HPLC. MK-2206 was purchased from Selleckchem (Houston, TX, USA). WKYMVm was obtained from Tocris Bioscience (Ellisville, MO, USA). FITC-labeled anti-CD11b, anti-Ly-6G, and anti-MPO antibodies were purchased from eBioscience (San Diego, CA, USA). The antibodies against p38 or $p47^{phox}$ and protein G beads were obtained from Santa Cruz Biotechnology (Santa Cruz, CA, USA). Anti-p-$p47^{phox}$ antibodies were from Abcam (Cambridge, MA, USA). Anti-PIP3 antibody was obtained from Echelon Biosciences (Salt Lake City, UT, USA). Other antibodies were purchased from Cell Signaling (Beverly, MA, USA). RPMI 1640, DMEM, L-glutamine, Antibiotic-Antimycotic dihydrorhodamine 123 (DHR123), *N*-formyl-Nle-Leu-Phe-Nle-Tyr-Lys (fNLFNYK), Alexa Fluor 594 Phalloidin, Hoechst 33342, were purchased from Thermo Fisher Scientific (Waltham, MA, USA). Fetal bovine serum (FBS) was from Biological Industries (Beth Haemek, Israel). Other regents were purchased from Sigma-Aldrich (St. Louis, MO, USA).

Neutrophil isolation

The procedure of neutrophil isolation was described previously (Chen et al, 2016; Hwang et al, 2009) and approved by the Institutional Review Board at Chang Gung Memorial Hospital. Neutrophils were isolated by dextran sedimentation and Ficoll-Hypaque centrifugation. Blood was from healthy volunteers (20-35 years old) and written informed consent was obtained from every volunteer. The purified neutrophils contained >98% viable cells, determined by trypan blue exclusion assay.

Cell culture and differentiation of HL-60 cells

Endothelial cells (ECs; bEnd.3) were obtained from the Bioresource Collection and Research Centre (Hsinchu, Taiwan) and cultured in DMEM media supplemented with 10% FBS, 1X Antibiotic-Antimycotic. The human promyelocytic leukemic HL-60 cell line was purchased from ATCC and cultured in RPMI 1640 media supplemented with 20% FBS, 2 mM L-glutamine, 1X Antibiotic-Antimycotic. Both cells were grown in a humidified atmosphere (37°C, 5% CO_2). The HL-60 cells were differentiated to neutrophil-like cells (dHL-60 cells) with a 5-day treatment of 1.3% DMSO in growth media.

Extracellular superoxide anion production

The activated neutrophils-produced superoxide anion was monitored using reduction of ferricytochrome *c* and described previously (Tsai et al, 2015b). In brief, human neutrophils ($6x10^5$ cells/ml) or dHL-60 cells ($1x10^6$ cells/ml) were equilibrated with 0.5 mg/ml ferricytochrome *c* and 1 mM Ca^{2+} at 37°C for 5 min. Cells were then preincubated with DMSO, CLLV-1 or MK-2206 and stimulated with fMLF, NaF, or WKYMVm before primed with cytochalasin B (CB; 1 or 2 μg/ml) for 3 min. The superoxide anion was determined by spectrophotometer (Hitachi, Tokyo, Japan) at 550 nm.

Intracellular ROS formation

DHR123 (2 μM)-labeled human neutrophils or dHL-60 cells ($1x10^6$ cells/ml) were incubated at 37°C for 10 min. Sequentially, cells were pretreated with DMSO or CLLV-1 for 5 min and activated by fMLF (0.1 μM)/CB (1 μg/ml) for another 5 min The intracellular ROS formation was determined by flow cytometry (BD Bioscience, San Jose, CA, USA).

Elastase release

Human neutrophils ($6x10^5$ cells/ml) were equilibrated with an elastase substrate (MeO-Suc-Ala-Ala-Pro-Val-p-nitroanilide, 100 μM) at 37°C for 5 min and then incubated with DMSO, CLLV-1 or MK-2206 for 5 min. Cells were then activated by fMLF, NaF, WKYMVm, IL-8, or LTB_4 for a further 10 min. CB (0.5 or 2 μg/ml) was added 3 min before stimulation. Elastase release was determined spectrophotometrically at 405 nm.

CD11b expression

Neutrophils ($5x10^6$ cells/ml) were preincubated with DMSO or CLLV-1 for 5 min and activated by fMLF (0.1 μM)/CB (0.5 μg/ml) for another 5 min. The cell pellets were then resuspended in 5% bovine serum albumin (BSA) containing FITC-labeled anti-CD11b antibodies (1 μg) at 4°C for 90 min. The fluorescent intensity was measured by flow cytometry.

Western blot

Human neutrophils were preincubated with DMSO or CLLV-1 at 37°C for 5 min and then activated by fMLF, NaF, WKYMVm, IL-8, or LTB_4 before primed with CB. The reaction was stopped by sample buffer (62.5 mM pH 6.8 Tris-HCl, 4% sodium dodecyl sulfate (SDS), 5% β-mercaptoethanol, 2.5 mM Na_3VO_4, 0.00125% bromophenol blue, 10 mM di-N-pentyl phthalate, and 8.75% glycerol) at 100°C for 15 min. The cell

lysates were separated by SDS-polyacrylamide gel electrophoresis (PAGE), and assayed by immunoblotting with the corresponding antibodies, followed by incubation with horseradish peroxidase-conjugated secondary anti-rabbit or anti-mouse antibodies. The labeled proteins were measured using an enhanced chemiluminescence system (Amersham Biosciences, Piscataway, NJ, USA).

PIP3 and F-actin expression

Neutrophils or dHL-60 cells ($5x10^6$ cells/ml) were preincubated with DMSO or CLLV-1 for 5 min and then activated by fMLF (0.1 μM)/CB (1 μg/ml). The reaction was stopped by 4% paraformaldehyde at 25°C for 20 min and then permeablized with 0.1% Triton-X-100. For F-actin staining, cells were incubated with Alexa Fluor 594 Phalloidin in HBSS containing 2% BSA at 25°C for 60 min. For PIP3 expression, cells were incubated with anti-PIP3 antibodies and FITC-labeled anti-mouse IgG antibodies in HBSS containing 2% BSA at 25°C for 60 min, respectively. The fluorescent intensity was monitored using flow cytometry.

Akt kinase assay

The Akt kinase activity was determined using the nonradioactive Akt kinase assay kit (Cell Signaling Technology, Beverly, MA, USA)) according to the manufacturer's protocol. In brief, dHL-60 cells were activated by fMLF (0.1 μM)/CB (1 μg/ml), and the active Akt in cell lysate was immunoprecipitated with immobilized Akt primary antibody. The precipitated Akt was treated with DMSO, CLLV-1 or MK-2206 at 30°C for 15 min and then incubated with ATP and GSK-3 fusion protein as a kinase substrate at 30°C for 30 min. The reaction was stopped by 3X SDS sample buffer at 100°C for 5 min. The phosphorylation of GSK-3 fusion protein was determined by Western blot.

Molecular docking

CLLV-1 was docked on Akt proteins by docking optimization (CDOCKER) and optimized with the CHARMm force field using Discovery Studio 4.1 (DS) (BIOVIA, San Diego, CA, USA). The binding of CLLV-1 and Akt1 with the most favorable energy is estimated with -CDOCKER (-kcal/mol). The crystal structure of Akt1 was obtained from PDB (accession code 4ekl) (Lin et al, 2012). The 3D structure of CLLV-1 was drawn by ChemDraw Ultra 9.0.

Nuclear magnetic resonance (NMR) spectrum analysis

CLLV-1 (1 mg) or synthetic Akt peptides (1 mg) were dissolved with 0.5 ml DMSO-*d6*. The mixtures of CLLV-1 (0.5 mg) and Akt peptides (1 mg) were vigorously mixed in 0.6 ml DMSO-*d6* and incubated at 25°C for 1 h. The ^{1}H NMR spectra were acquired

by using a Bruker AVANCE-400MHz FT-NMR spectrometer (Bruker BioSpin GmbH, Billerica, MA, USA).

Mass spectrometry (MS) analysis

Synthetic Akt peptides were dissolved with phosphate-buffered saline (PBS). The mixtures of Akt peptides (120 μM) and CLLV-1 (60 μM) were incubated at 25°C for 2 h. The Akt peptides and their CLLV-1 adducts were detected using matrix-assisted laser desorption/ionization time of flight mass spectrometer (MALDI-TOF MS). The Akt peptides and their CLLV-1 adducts were mixed with CHCA matrix (2 mg/ml in 80% acetonitrile containing 0.1% trichloroacetic acid) and loaded onto a MTP AnchorChip™ 600/384 TF (Bruker Daltonik GmbH, Bremen, Germany). After the crystallization of the peptides and the matrix, the samples were analyzed by an Ultraflex™ MALDI-TOF MS (Bruker Daltonik GmbH, Bremen, Germany) controlled by the FlexControl software (v.2.2; Bruker Daltonics, Bremen, Germany). Data processing was performed and monoisotopic peptide mass was acquired using the FlexAnalysis 2.4 peak-picking software (Bruker Daltonics, Bremen, Germany).

AMS labeling assay

The redox states of the proteins were examined by conjugating free thiol with 4-acetamido-4'-maleimidylstilbene-2,2'-disulfonic acid (AMS) (Ahmad et al, 2014). The cells were lysed in the buffer (50 mM Tris, pH 7.4, 150 mM NaCl, 0.5% Triton-X-100, 1X protease inhibitor cocktail) and centrifuged at 12,000 g for 10 min. The supernatants were incubated with 30 mM AMS at 4°C for 24 h and then mixed with non-reducing sample buffer (62.5 mM pH 6.8 Tris-HCl, 4% SDS, 0.00125% bromophenol blue and 8.75% glycerol) at 37°C for 10 min. The redox states of the proteins were determined by immunoblotting.

Immunoprecipitation

Cells were lysed in the buffer (50 mM Tris, pH 7.4, 150 mM NaCl, 0.5% Triton X-100, 1X protease inhibitor cocktail) and centrifuged at 12,000 g for 10 min. The supernatants were incubated with protein G beads bound with Akt antibodies. The beads were washed with buffer and the precipitated proteins were assayed by immunoblotting.

Neutrophil adhesion assay

The bEnd.3 endothelial cells (ECs) were activated with LPS (2 μg/ml) for 4 h. Hoechst 33342-labeled neutrophils were preincubated with DMSO or CLLV-1 for 5 min and activated by fMLF (0.1 μM)/CB (1 μg/ml) for another 5 min. Activated neutrophils were

then co-cultured with LPS-pre-activated bEnd.3 ECs for 30 min. After gently washing, adherent neutrophils on bEnd.3 ECs were randomly counted in 4 fields by microscopy (IX81, Olympus, Center Valley, PA, USA).

Chemotactic migration assay

Human neutrophil chemotactic migration assay was described previously (Chen et al, 2015). Briefly, DMSO- or CLLV-1-pretreated neutrophils on the top microchemotaxis chamber (Merck Millipore, Darmstadt, Germany) were placed into the bottom well containing 0.1 μM fMLF. After 90 min, the migrated neutrophils were counted.

LPS-induced acute lung injury (ALI)

The 7-8 weeks old C57BL/6 male mice were intraperitoneally injected with CLLV-1 (10 mg/kg), MK-2206 (10 mg/kg) or an equal volume of the DMSO. After 1 h, the tracheostomy procedure was performed under anesthesia. Mice were instilled with 2 mg/kg LPS (*Escherichia coli* 0111:B4) or 0.9% saline. After 6 h, the lungs were fixed in 10% formalin for immunohistochemistry or frozen for MPO activity.

Myeloperoxidase (MPO) activity

The lung tissues were immersed in 10 mM PBS, pH 6.0, with 0.5% hexadecyltrimethylammonium bromide and sonicated by a homogenizer. The MPO activity was determined using MPO substrate buffer (PBS, pH 6.0, 0.2 mg/mL o-dianisidine hydrochloride and 0.001% hydrogen peroxide) and monitored the absorbance at 405 nm by a spectrometer. The serial concentration of human MPO was used as a standard curve to calculate the MPO activity. Total protein levels were measured by Bradford Protein Assay (Bio-rad, Hercules, CA, USA). The final MPO activity was normalized to the corresponding protein concentration (U/mg).

Immunohistochemistry (IHC)

Formalin-fixed paraffin embedded tissue sections were used for IHC. All slides were stained with hematoxylin and eosin (H&E) for morphologic determination. The anti-MPO antibodies, anti-Ly6G antibodies, anti-pAkt (S473) antibodies or the SuperPicture kit (Thermo Fisher Scientific, Waltham, MA, USA) were used as the primary or secondary antibodies, following a previously published protocol by Pathology Core of Chang Gung University (Yuan et al, 2006).

Complete Freund's adjuvant (CFA)-induced paw edema

The 7–8 weeks old C57BL/6 male mice were intraperitoneally injected with CLLV-1 (5 or 10 mg/kg), MK-2206 (10 mg/kg) or an equal volume of the DMSO. After 1 h, paw

inflammation was initiated by intraplantar injection with 30 µl CFA (1 mg/ml *Mycobacterium tuberculosis*, 85% paraffin oil and 15% mannide monooleate) or 0.9% saline. The paw thickness was determined by a digital caliper (INSIZE, Vienna, Austria) before CFA injection (baseline) or after CFA/saline injection at the indicated times. Paw edema was expressed as the change of thickness (mm) (Tsai et al, 2015a).

Statistical analysis

Data are presented as means ± S.E.M. Statistical analysis was performed with SigmaPlot (Systat Software) using Student's *t*-test. $P < 0.05$ was considered statistically significant.

The paper explained

Problem

Akt controls the inflammatory responses of neutrophils; however, the regulatory mechanism of Akt in neutrophil remains elusive, especially in redox modification. As well, development of Akt inhibitors for neutrophilic inflammation therapy is still inadequate.

Results

CLLV-1 inhibits the Akt activity and attenuates the inflammatory responses in human neutrophils, including respiratory burst, degranulation, and chemotaxis. CLLV-1 targets Cys310 in catalytic domain of Akt through thiol-based reaction. Targeting the redox modification of Akt also alleviates inflammatory responses of LPS-induced ALI and CFA-caused inflammatory arthritis in mice.

Impact

This is the first study to demonstrate that pharmacologically targeting Akt Cys310 can restrict neutrophilic inflammation. CLLV-1 is identified as a novel covalent-allosteric Akt inhibitor via targeting Akt Cys310 to retrain Akt activity and inflammatory responses in human neutrophils and in inflammatory animals. Our findings sustain a preclinical characterization of Akt redox modification that may be a novel pharmacological target to alleviate neutrophilic inflammation.

Acknowledgments

This research was financial supported by the grants from the Ministry of Science Technology (MOST 106-2320-B-255-003-MY3 and MOST 104-2320-B-255-004-MY3), Ministry of Education (EMRPD1G0231), and Chang Gung Memorial Hospital (CMRPF1F0011~3, CMRPF1F0061~3, and BMRP450), Taiwan. The funders had no role in study design, data collection and analysis, decision to publish, or preparation of the manuscript.

Author contribution

P.-J.C. designed and performed most experiments. I.-L. K., C.-L. L., F.-R. C., Y.-C. Wu., Y.-L. L., C.-C. W., Y.-F. T., C.-Y. Lin. and C.-Y. P. helped to perform experiments and analyzed the data. C.-L. L., H.-C. H., F.-R. C. and Y.-C. W. isolated and provide CLLV-1. P.-J.C. and T.-L.H. wrote and completed the manuscript. T.-L.H. supervised the entire study.

Conflict of interest

The authors declare no conflicts of interest exist.

References

Ahmad F, Nidadavolu P, Durgadoss L, Ravindranath V (2014) Critical cysteines in Akt1 regulate its activity and proteasomal degradation: implications for neurodegenerative diseases. Free radical biology & medicine 74**:** 118-128

Aschner Y, Zemans RL, Yamashita CM, Downey GP (2014) Matrix metalloproteinases and protein tyrosine kinases: potential novel targets in acute lung injury and ARDS. Chest 146**:** 1081-1091

Brazil DP, Yang ZZ, Hemmings BA (2004) Advances in protein kinase B signalling: AKTion on multiple fronts. Trends in biochemical sciences 29**:** 233-242

Chamcheu JC, Adhami VM, Esnault S, Sechi M, Siddiqui IA, Satyshur KA, Syed DN, Dodwad SM, Chaves-Rodriquez MI, Longley BJ et al (2017) Dual Inhibition of PI3K/Akt and mTOR by the Dietary Antioxidant, Delphinidin, Ameliorates Psoriatic Features In Vitro and in an Imiquimod-Induced Psoriasis-Like Disease in Mice. Antioxidants & redox signaling 26**:** 49-69

Chen CY, Leu YL, Fang Y, Lin CF, Kuo LM, Sung WC, Tsai YF, Chung PJ, Lee MC, Kuo YT et al (2015) Anti-inflammatory effects of Perilla frutescens in activated human neutrophils through two independent pathways: Src family kinases and Calcium. Scientific reports 5**:** 18204

Chen J, Tang H, Hay N, Xu J, Ye RD (2010) Akt isoforms differentially regulate neutrophil functions. Blood 115**:** 4237-4246

Chen PJ, Wang YL, Kuo LM, Lin CF, Chen CY, Tsai YF, Shen JJ, Hwang TL (2016) Honokiol suppresses TNF-alpha-induced neutrophil adhesion on cerebral endothelial cells by disrupting polyubiquitination and degradation of IkappaBalpha. Scientific reports 6**:** 26554

Chen Q, Powell DW, Rane MJ, Singh S, Butt W, Klein JB, McLeish KR (2003) Akt phosphorylates p47phox and mediates respiratory burst activity in human neutrophils. Journal of immunology 170**:** 5302-5308

Chodniewicz D, Zhelev DV (2003) Novel pathways of F-actin polymerization in the human neutrophil. Blood 102**:** 2251-2258

Corcoran A, Cotter TG (2013) Redox regulation of protein kinases. The FEBS journal 280**:** 1944-1965

Delano MJ, Ward PA (2016) Sepsis-induced immune dysfunction: can immune therapies reduce mortality? The Journal of clinical investigation 126**:** 23-31

Dennehy MK, Richards KA, Wernke GR, Shyr Y, Liebler DC (2006) Cytosolic and nuclear protein targets of thiol-reactive electrophiles. Chemical research in toxicology 19**:** 20-29

Dorward DA, Lucas CD, Chapman GB, Haslett C, Dhaliwal K, Rossi AG (2015) The role of formylated peptides and formyl peptide receptor 1 in governing neutrophil function during acute inflammation. The American journal of pathology 185**:** 1172-1184

Durgadoss L, Nidadavolu P, Valli RK, Saeed U, Mishra M, Seth P, Ravindranath V (2012) Redox modification of Akt mediated by the dopaminergic neurotoxin MPTP, in mouse midbrain, leads to down-regulation of pAkt. FASEB journal : official publication of the Federation of American Societies for Experimental Biology 26**:** 1473-1483

El-Benna J, Dang PM, Gougerot-Pocidalo MA, Marie JC, Braut-Boucher F (2009) p47phox, the phagocyte NADPH oxidase/NOX2 organizer: structure, phosphorylation and implication in diseases. Experimental & molecular medicine 41**:** 217-225

El-Benna J, Hurtado-Nedelec M, Marzaioli V, Marie JC, Gougerot-Pocidalo MA, Dang PM (2016) Priming of the neutrophil respiratory burst: role in host defense and inflammation. Immunological reviews 273**:** 180-193

Futosi K, Fodor S, Mocsai A (2013) Reprint of Neutrophil cell surface receptors and their intracellular signal transduction pathways. International immunopharmacology 17**:** 1185-1197

Galli S, Antico Arciuch VG, Poderoso C, Converso DP, Zhou Q, Bal de Kier Joffe E, Cadenas E, Boczkowski J, Carreras MC, Poderoso JJ (2008) Tumor cell phenotype is sustained by selective MAPK oxidation in mitochondria. PloS one 3**:** e2379

Heerding DA, Rhodes N, Leber JD, Clark TJ, Keenan RM, Lafrance LV, Li M, Safonov

IG, Takata DT, Venslavsky JW et al (2008) Identification of 4-(2-(4-amino-1,2,5-oxadiazol-3-yl)-1-ethyl-7-{[(3S)-3-piperidinylmethyl]oxy}-1H-imidazo[4,5-c]pyridin-4-yl)-2-methyl-3-butyn-2-ol (GSK690693), a novel inhibitor of AKT kinase. Journal of medicinal chemistry 51**:** 5663-5679

Hirai H, Sootome H, Nakatsuru Y, Miyama K, Taguchi S, Tsujioka K, Ueno Y, Hatch H, Majumder PK, Pan BS et al (2010) MK-2206, an allosteric Akt inhibitor, enhances antitumor efficacy by standard chemotherapeutic agents or molecular targeted drugs in vitro and in vivo. Molecular cancer therapeutics 9**:** 1956-1967

Hoenderdos K, Lodge KM, Hirst RA, Chen C, Palazzo SG, Emerenciana A, Summers C, Angyal A, Porter L, Juss JK et al (2016) Hypoxia upregulates neutrophil degranulation and potential for tissue injury. Thorax 71**:** 1030-1038

Hoyal CR, Gutierrez A, Young BM, Catz SD, Lin JH, Tsichlis PN, Babior BM (2003) Modulation of p47PHOX activity by site-specific phosphorylation: Akt-dependent activation of the NADPH oxidase. Proceedings of the National Academy of Sciences of the United States of America 100**:** 5130-5135

Hwang TL, Li GL, Lan YH, Chia YC, Hsieh PW, Wu YH, Wu YC (2009) Potent inhibition of superoxide anion production in activated human neutrophils by isopedicin, a bioactive component of the Chinese medicinal herb Fissistigma oldhamii. Free radical biology & medicine 46**:** 520-528

Jacinto E, Lorberg A (2008) TOR regulation of AGC kinases in yeast and mammals. The Biochemical journal 410**:** 19-37

Jorch SK, Kubes P (2017) An emerging role for neutrophil extracellular traps in noninfectious disease. Nature medicine 23**:** 279-287

Keane NA, Glavey SV, Krawczyk J, O'Dwyer M (2014) AKT as a therapeutic target in multiple myeloma. Expert opinion on therapeutic targets 18**:** 897-915

Kim K, Li J, Barazia A, Tseng A, Youn SW, Abbadessa G, Yu Y, Schwartz B, Andrews RK, Gordeuk VR et al (2017) ARQ 092, an orally-available, selective AKT inhibitor, attenuates neutrophil-platelet interactions in sickle cell disease. Haematologica 102**:** 246-259

Kumar S, Xu J, Kumar RS, Lakshmikanthan S, Kapur R, Kofron M, Chrzanowska-Wodnicka M, Filippi MD (2014) The small GTPase Rap1b negatively regulates neutrophil chemotaxis and transcellular diapedesis by inhibiting Akt activation. The Journal of experimental medicine 211**:** 1741-1758

Lame MW, Jones AD, Wilson DW, Segall HJ (2003) Protein targets of 1,4-benzoquinone and 1,4-naphthoquinone in human bronchial epithelial cells. Proteomics 3**:** 479-495

Lee CL, Lin YT, Chang FR, Chen GY, Backlund A, Yang JC, Chen SL, Wu YC (2012) Synthesis and biological evaluation of phenanthrenes as cytotoxic agents with pharmacophore modeling and ChemGPS-NP prediction as topo II inhibitors. PloS one 7**:** e37897

Lee CL, Nakagawa-Goto K, Yu D, Liu YN, Bastow KF, Morris-Natschke SL, Chang FR, Wu YC, Lee KH (2008) Cytotoxic calanquinone A from Calanthe arisanensis and its first total synthesis. Bioorganic & medicinal chemistry letters 18**:** 4275-4277

Lee CL, Yen MH, Chang FR, Wu CC, Wu YC (2014) Antiplatelet aggregation effects of phenanthrenes from Calanthe arisanensis. Natural product communications 9**:** 83-84

Lee JY, Lee YG, Lee J, Yang KJ, Kim AR, Kim JY, Won MH, Park J, Yoo BC, Kim S et al (2010) Akt Cys-310-targeted inhibition by hydroxylated benzene derivatives is tightly linked to their immunosuppressive effects. The Journal of biological chemistry 285**:** 9932-9948

Lee YS, Park JS, Jung SM, Kim SD, Kim JH, Lee JY, Jung KC, Mamura M, Lee S, Kim SJ et al (2015) Inhibition of lethal inflammatory responses through the targeting of membrane-associated Toll-like receptor 4 signaling complexes with a Smad6-derived peptide. EMBO molecular medicine 7**:** 577-592

Leiding JW (2017) Neutrophil Evolution and Their Diseases in Humans. Frontiers in immunology 8**:** 1009

Ley K, Laudanna C, Cybulsky MI, Nourshargh S (2007) Getting to the site of inflammation: the leukocyte adhesion cascade updated. Nature reviews Immunology 7**:** 678-689

Li J, Kim K, Hahm E, Molokie R, Hay N, Gordeuk VR, Du X, Cho J (2014) Neutrophil AKT2 regulates heterotypic cell-cell interactions during vascular inflammation. The Journal of clinical investigation 124**:** 1483-1496

Lin K, Lin J, Wu WI, Ballard J, Lee BB, Gloor SL, Vigers GP, Morales TH, Friedman LS, Skelton N et al (2012) An ATP-site on-off switch that restricts phosphatase accessibility of Akt. Science signaling 5**:** ra37

Liu J, Qian C, Cao X (2016) Post-Translational Modification Control of Innate Immunity. Immunity 45**:** 15-30

Luanpitpong S, Chanvorachote P, Nimmannit U, Leonard SS, Stehlik C, Wang L, Rojanasakul Y (2012) Mitochondrial superoxide mediates doxorubicin-induced keratinocyte apoptosis through oxidative modification of ERK and Bcl-2 ubiquitination. Biochemical pharmacology 83**:** 1643-1654

Manning BD, Toker A (2017) AKT/PKB Signaling: Navigating the Network. Cell 169**:** 381-405

Mi L, Hood BL, Stewart NA, Xiao Z, Govind S, Wang X, Conrads TP, Veenstra TD, Chung FL (2011) Identification of potential protein targets of isothiocyanates by proteomics. Chemical research in toxicology 24**:** 1735-1743

Murata H, Ihara Y, Nakamura H, Yodoi J, Sumikawa K, Kondo T (2003) Glutaredoxin exerts an antiapoptotic effect by regulating the redox state of Akt. The Journal of biological chemistry 278**:** 50226-50233

Nanamori M, Chen J, Du X, Ye RD (2007) Regulation of leukocyte degranulation by cGMP-dependent protein kinase and phosphoinositide 3-kinase: potential roles in phosphorylation of target membrane SNARE complex proteins in rat mast cells. Journal of immunology 178**:** 416-427

Nauseef WM, Borregaard N (2014) Neutrophils at work. Nature immunology 15**:** 602-611

Nicolas-Avila JA, Adrover JM, Hidalgo A (2017) Neutrophils in Homeostasis, Immunity, and Cancer. Immunity 46**:** 15-28

Nitulescu GM, Margina D, Juzenas P, Peng Q, Olaru OT, Saloustros E, Fenga C, Spandidos D, Libra M, Tsatsakis AM (2016) Akt inhibitors in cancer treatment: The long journey from drug discovery to clinical use (Review). International journal of oncology 48**:** 869-885

Ortega-Gomez A, Perretti M, Soehnlein O (2013) Resolution of inflammation: an integrated view. EMBO molecular medicine 5**:** 661-674

Shearn CT, Reigan P, Petersen DR (2012) Inhibition of hydrogen peroxide signaling by 4-hydroxynonenal due to differential regulation of Akt1 and Akt2 contributes to decreases in cell survival and proliferation in hepatocellular carcinoma cells. Free radical biology & medicine 53**:** 1-11

Soehnlein O, Steffens S, Hidalgo A, Weber C (2017) Neutrophils as protagonists and targets in chronic inflammation. Nature reviews Immunology 17**:** 248-261

Sousa LP, Lopes F, Silva DM, Tavares LP, Vieira AT, Rezende BM, Carmo AF, Russo RC, Garcia CC, Bonjardim CA et al (2010) PDE4 inhibition drives resolution of neutrophilic inflammation by inducing apoptosis in a PKA-PI3K/Akt-dependent and NF-kappaB-independent manner. Journal of leukocyte biology 87**:** 895-904

Tsai YF, Yang SC, Hwang TL (2016) Formyl peptide receptor modulators: a patent review and potential applications for inflammatory diseases (2012-2015). Expert opinion on therapeutic patents**:** 1-18

Tsai YF, Yu HP, Chang WY, Liu FC, Huang ZC, Hwang TL (2015a) Sirtinol inhibits neutrophil elastase activity and attenuates lipopolysaccharide-mediated acute lung injury in mice. Scientific reports 5**:** 8347

Tsai YF, Yu HP, Chung PJ, Leu YL, Kuo LM, Chen CY, Hwang TL (2015b) Osthol attenuates neutrophilic oxidative stress and hemorrhagic shock-induced lung injury via inhibition of phosphodiesterase 4. Free radical biology & medicine 89**:** 387-400

Weichhart T, Hengstschlager M, Linke M (2015) Regulation of innate immune cell function by mTOR. Nature reviews Immunology 15**:** 599-614

Yang SC, Hwang TL (2016) The potential impacts of formyl peptide receptor 1 in inflammatory diseases. Frontiers in bioscience 8**:** 436-449

Yuan P, Temam S, El-Naggar A, Zhou X, Liu DD, Lee JJ, Mao L (2006) Overexpression of podoplanin in oral cancer and its association with poor clinical outcome. Cancer 107**:** 563-569

Zeng T, Zhang CL, Zhao N, Guan MJ, Xiao M, Yang R, Zhao XL, Yu LH, Zhu ZP, Xie KQ (2018) Impairment of Akt activity by CYP2E1 mediated oxidative stress is involved in chronic ethanol-induced fatty liver. Redox biology 14**:** 295-304

Zhang Y, Wang X, Yang H, Liu H, Lu Y, Han L, Liu G (2013) Kinase AKT controls innate immune cell development and function. Immunology 140**:** 143-152

Figure legends

Figure 1. CLLV-1 attenuates the superoxide anion generation, ROS formation, and p47^{phox} phosphorylation in fMLF-activated human neutrophils.

A The chemical structure of CLLV-1.

B-C Human neutrophils were preincubated with DMSO or CLLV-1 (0.03-3 μM) and then activated with or without fMLF (0.1 μM)/CB (1 μg/ml). (B) Superoxide anion generation was detected using cytochrome *c* reduction by spectrophotometer at 550 nm. (C) The intracellular ROS was monitored using cell permeable DHR123 by flow cytometry.

D Phosphorylation of p47^{phox} was analyzed by immunoblotting using antibodies against the phosphorylated (S304) and total p47^{phox}.

Data information: All data are expressed as the mean ± S.E.M. (n=3), *$p < 0.05$, **$p < 0.01$, ***$p < 0.001$ compared with the DMSO + fMLF (Student's *t*-test).

Figure 2. CLLV-1 inhibits the elastase release, CD11b/F-actin expression, and neutrophil adhesion/migration in fMLF-activated human neutrophils.

A-C Human neutrophils were incubated with DMSO or CLLV-1 (0.3-3 μM) for 5 min before stimulation with or without fMLF (0.1 μM)/CB (0.5 or 1 μg/ml). (A) Elastase release was measured using elastase substrate by spectrophotometer at 405 nm. (B) The CD11b levels on cell surface were detected using FITC-labeled anti-CD11b antibodies by flow cytometry. (C) The F-actin levels were assayed using Alexa Fluor 594 Phalloidin by flow cytometry.

D Hoechst 33342-labeled neutrophils were pretreated with DMSO or CLLV-1 (0.1-3 μM) for 5 min and stimulated with fMLF (0.1 μM)/CB (1 μg/ml). Sequentially, neutrophils were incubated with LPS-preactivated ECs for another 30 min. After gently washing, ECs-associated neutrophils were counted using microscopy.

E Neutrophils were preincubated with DMSO or CLLV-1 (0.3-3 μM) for 5 min in the top chamber. Migrated neutrophils in the bottom wells with or without fMLF were counted after 90 min.

Data information: All data are expressed as the mean ± S.E.M. (n=3), *$p < 0.05$, **$p < 0.01$, ***$p < 0.001$ compared with the DMSO + fMLF (Student's *t*-test).

Figure 3. CLLV-1 decreases the phosphorylation of Akt but not MAPKs in fMLF-activated human neutrophils.

A-D Human neutrophils were incubated with CLLV-1 (0.3-3 μM) for 5 min before stimulation with or without fMLF (0.1 μM)/CB (1 μg/ml). Phosphorylation of (A) Akt, (B) ERK, (C) JNK or (D) p38 MAPK was analyzed by immunoblotting using antibodies

against the phosphorylated form and the total of each protein.

Data information: All data are expressed as the mean ± S.E.M. (n=3), ***p < 0.001 compared with the DMSO + fMLF (Student's *t*-test).

Figure 4. CLLV-1 suppresses the fMLF-induced inflammatory responses in differentiated HL-60 (dHL-60) cells.

A The HL-60 cells were exposed to 1.3% DMSO for 5 days. The differentiation of HL-60 cells by DMSO was examined using anti-FPR1 antibodies by flow cytometry.

B-F The dHL-60 cells were preincubated with DMSO or CLLV-1 (0.03-1 μM) and then activated with or without fMLF (0.1 μM)/CB (1 μg/ml). (B) Superoxide anion generation was detected using cytochrome *c* reduction by spectrophotometer at 550. (C) The intracellular ROS was monitored using cell permeable DHR123 by flow cytometry. (D) Phosphorylation of $p47^{phox}$ was analyzed by immunoblotting using antibodies against the phosphorylated (S304) and the total $p47^{phox}$. (E) The F-actin levels were assayed using Alexa Fluor 594 Phalloidin by flow cytometry. (F) Phosphorylation of Akt was analyzed by immunoblotting using antibodies against the phosphorylated (S473 and T308) and total Akt.

Data information: All data are expressed as the mean ± S.E.M. (n=3), *p < 0.05, **p < 0.01, ***p < 0.001 compared with the DMSO + fMLF (Student's *t*-test).

Figure 5. CLLV-1 blocks the Akt enzymatic activity but not affect the Akt upstream kinase.

A-B dHL-60 cells were preincubated with DMSO or CLLV-1 (0.03-1 μM) and then activated with or without fMLF (0.1 μM)/CB (1 μg/ml). (A) Phosphorylations of Akt upstream kinases, PDK1, mTORC2, and PI3K were determined by immunoblotting using antibodies against the phosphorylated form and normalized with GAPDH. (B) The PIP3 levels were assayed using anti-PIP3 antibodies by flow cytometry.

C The active Akt proteins were immunoprecipitated using phospho-Akt antibodies and treated with DMSO or CLLV-1 (0.3-3 μM) for 15 min at 30°C. Sequentially, GSK-3 Fusion Protein (Akt substrate) was added for another 30 min. The phospho-GSK-3 Fusion Protein was examined by immunoblotting.

D The phosphorylation of GSK-3 Fusion Protein was quantified, expressed as a percentage to represent Akt kinase activity.

Data information: All data are expressed as the mean ± S.E.M. (n=3), *p < 0.05, ***p < 0.001 compared with the DMSO + Akt (Student's *t*-test).

Figure 6. CLLV-1 covalently reacts with the cysteine thiol of Akt *in vitro*.

A-B Docking models of CLLV-1-targeted Akt. Surface presentation demonstrates the

structure of Akt (gray). CLLV-1 moieties are colored green and rendered in stick representation (A). Close-up of CLLV-1 docking site (best energy mode) (B). The figures were prepared by using Discovery Studio 4.1. The crystal structure of Akt was downloaded from PDB (accession code 4ekl). The chemical structure of CLLV-1 was drawn by ChemDraw Ultra 9.0.

C ^{1}H NMR spectra of CLLV-1 (upper panel), synthetic Akt peptide ($Akt_{309-313}$; FCGTP) (middle panel) and mixtures of CLLV-1 and $Akt_{309-313}$ (lower panel).

D-E The synthetic Akt peptides, $Akt_{309-313}$ or $Akt_{307-328}$ (KTFCGTPEYLAPEVLEDNDYGR), were incubated in the presence or absence of CLLV-1. The molecular mass of the synthetic Akt peptides and their CLLV-1 adducts are detected using MALDI-TOF MS. M, molecular mass of Akt peptides; M_{CLL}, molecular mass of adducts of Akt peptides and CLLV-1.

Figure 7. CLLV-1 decreases the AMS-labeled reduced form of Akt and increases the Akt-PP2A interaction in fMLF-activated dHL-60 cells.

dHL-60 cells were incubated with CLLV-1 (0.3-3 μM) for 5 min before stimulation with or without fMLF (0.1 μM)/CB (1 μg/ml).

A The cell lysates were incubated with the thiol alkylating agent AMS for 12 h on ice and analyzed by Western blotting under reducing (total lysate) or non-reducing conditions (AMS-labeled Akt). The AMS-labeled reduced form of Akt (Red) showed higher molecular weight than oxidized Akt (Oxi).

B The cell lysates were immunoprecipitated with control (Ctrl) or Akt IgG. The precipitated substances were used for Western blotting of Akt and PP2A.

Figure 8. CLLV-1 attenuates the LPS-induced ALI in mice. C57BL/6 mice were intraperitoneally injected with CLLV-1 (10 mg/kg), MK-2206 (10 mg/kg) or an equal volume of the DMSO for 1 h, and following instilled 2 mg/kg LPS from *E. coli* 0111:B4 or 0.9% saline via the tracheostomy.

A-B 6 hours later, lungs were collected and assayed for MPO activity (A) and protein levels (B).

C Histological examination of lungs. The lung sections were stained with hematoxylin and eosin (H&E), anti-Ly6G antibodies or anti-pAkt (S473) antibodies by IHC.

Data information: All data are expressed as mean ± S.E.M. (n=6), $^{**}p < 0.01$, $^{***}p < 0.001$ compared with the LPS + DMSO; $^{\#\#\#}p < 0.001$ compared with the DMSO control. (Student's *t*-test).

Figure 9. Schematic model of CLLV-1-impeded neutrophilic inflammation.

With stimulation, Akt is activated and phosphorylated, leading to PH domain distant from the kinase domain. Active Akt is maintained in a reduced manner that contributes overwhelming inflammatory responses in human neutrophils and neutrophil-dominant inflammatory disorders. Once CLLV-1 exists, it covalently binds to Cys310 within the kinase domain of Akt to cause inactive and less reduced form of Akt. CLLV-1 can inhibit neutrophil activations, including respiratory burst, degranulation, and chemotaxis via redoxically targeting Akt. As well, CLLV-1 ameliorates the inflammatory disorders such as ALI and inflammatory arthritis in mice.

Expanded View Figure Legends

Figure EV1. CLLV-1 represses superoxide anion generation or elastase release in NaF-, WKYMVm-, IL-8 or LTB_4-activated human neutrophils.

A-F Human neutrophils were preincubated with DMSO or CLLV-1 (0.03-3 μM) and then activated with or without (A,C) NaF (20 mM)/CB (2 μg/ml), (B,D) WKYMVm (1 nM)/CB (1 μg/ml), (E) IL-8 (50 ng/ml)/CB (2 μg/ml) or (F) LTB_4 (0.1 μM)/CB (0.5 μg/ml). Superoxide anion generation (A,B) and elastase release (C-F) were assayed using cytochrome *c* reduction and elastase substrate by spectrophotometer at 550 nm and 405 nm, respectively.

Data information: All data are expressed as the mean ± S.E.M. (n=3), $^{**}p < 0.01$, $^{***}p < 0.001$ compared with the DMSO + fMLF (Student's *t*-test).

Figure EV2. CLLV-1 inhibits the phosphorylation of Akt in NaF-, WKYMVm-, IL-8 or LTB_4-activated human neutrophils.

A-D Human neutrophils were preincubated with DMSO or CLLV-1 (0.03-3 μM) and then activated with or without (A) NaF (20 mM)/CB (2 μg/ml), (B) WKYMVm (1 nM)/CB (1 μg/ml), (C) IL-8 (50 ng/ml)/CB (2 μg/ml) or (D) LTB_4 (0.1 μM)/CB (0.5 μg/ml). Phosphorylation of Akt was analyzed by immunoblotting using antibodies against the phosphorylated (S473 and T308) and total Akt.

Data information: All data are expressed as the mean ± S.E.M. (n=3), $^{*}p < 0.05$, $^{**}p < 0.01$, $^{***}p < 0.001$ compared with the DMSO + fMLF (Student's *t*-test).

Figure EV3. MK-2206 suppresses superoxide anion generation and elastase release in fMLF-activated human neutrophils and Akt activity *in vitro*.

Human neutrophils were preincubated with DMSO or MK-2206 (0.3-10 μM) and then activated with or without fMLF (0.1 μM)/CB (1 μg/ml).

A Superoxide anion generation was detected using cytochrome *c* reduction by spectrophotometer at 550 nm.

B Elastase release was measured at 405 nm.

C The active Akt proteins were immunoprecipitated with phospho-Akt antibodies and treated with DMSO, CLLV-1 (1 or 3 μM) or MK-2206 (0.3-3μM) for 15 min at 30°C following GSK-3 fusion protein (Akt substrate) for another 30 min. The phospho-GSK-3 fusion protein was examined by immunoblotting.

Data information: All data are expressed as the mean ± S.E.M. (n=3), $^{*}p < 0.05$, $^{**}p < 0.01$, $^{***}p < 0.001$ compared with the DMSO + fMLF (A or B) or GSK protein + Akt (C) (Student's *t*-test).

Figure EV4. The chemical interaction of CLLV-1 and synthetic Akt peptides.

A ^{1}H NMR spectra of CLLV-1, synthetic Akt peptides (304-308 or 314-318), and mixtures of CLLV-1 and Akt peptides.

B The synthetic Akt peptides, $Akt_{304-308}$ or $Akt_{314-318}$, were incubated in the presence or absence of CLLV-1. The molecular mass of the synthetic Akt peptides and their CLLV-1 adducts were detected using MALDI-TOF MS. M, molecular mass of Akt peptides.

Figure EV5. CLLV-1 represses CFA-induced paw inflammation in mice. C57BL/6 mice were intraperitoneally injected with CLLV-1 (5 mg/kg or 10 mg/kg), MK-2206 (10 mg/kg) or an equal volume of the DMSO for 1h, and following injected with 30 μl of CFA or 0.9% saline into the intraplantar space in the hind paw.

A The thickness of the paw was determined using a digital Vernier caliper at the indicated times.

B The infiltrated neutrophils in paw were stained with anti-Ly6G and anti-MPO antibodies by IHC.

Data information: All data are expressed as mean ± S.E.M. (n=6), $^{**}p < 0.01$, $^{***}p < 0.001$ compared with the CFA + DMSO (Student's *t*-test).

Figure 1

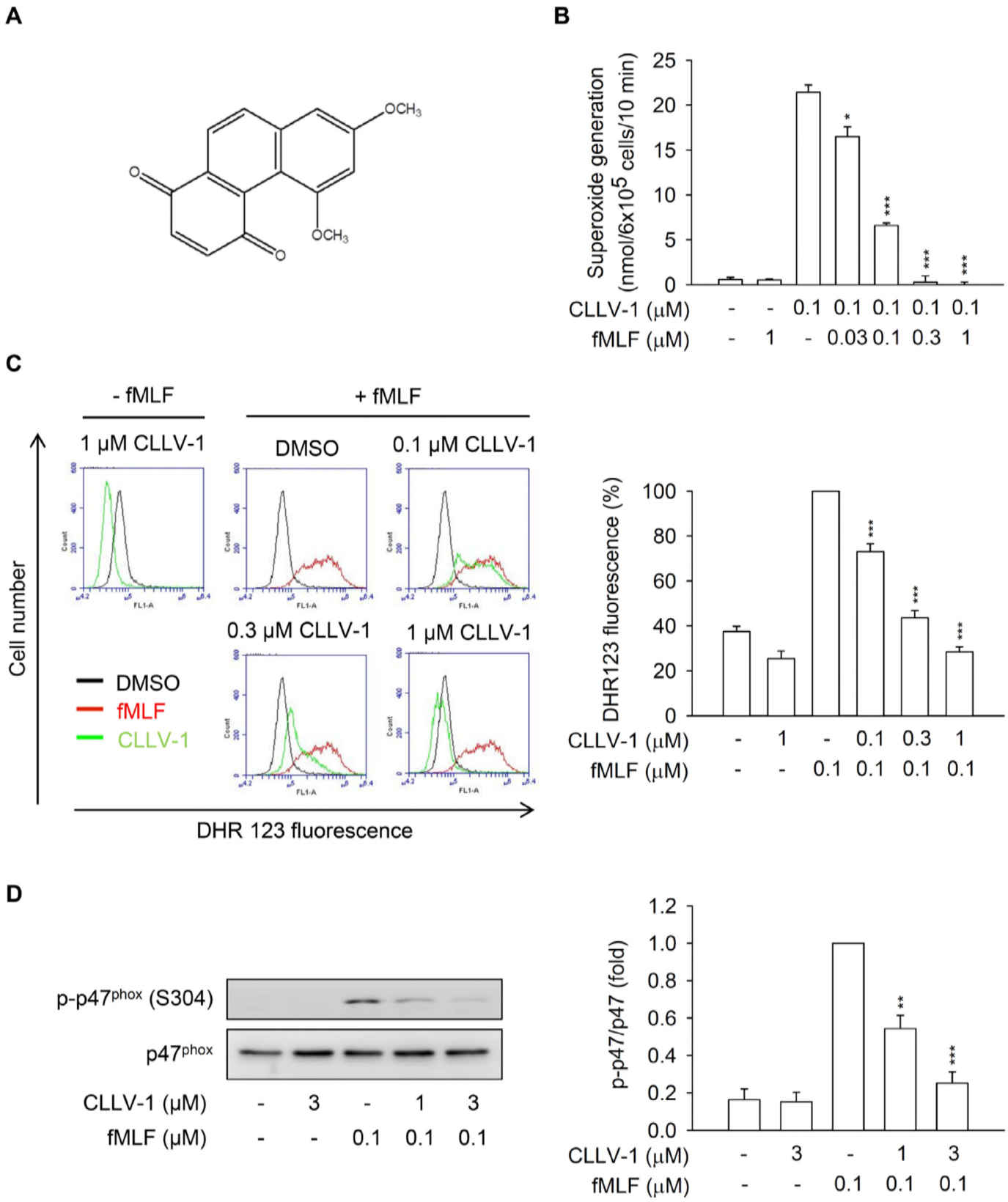

Figure 2

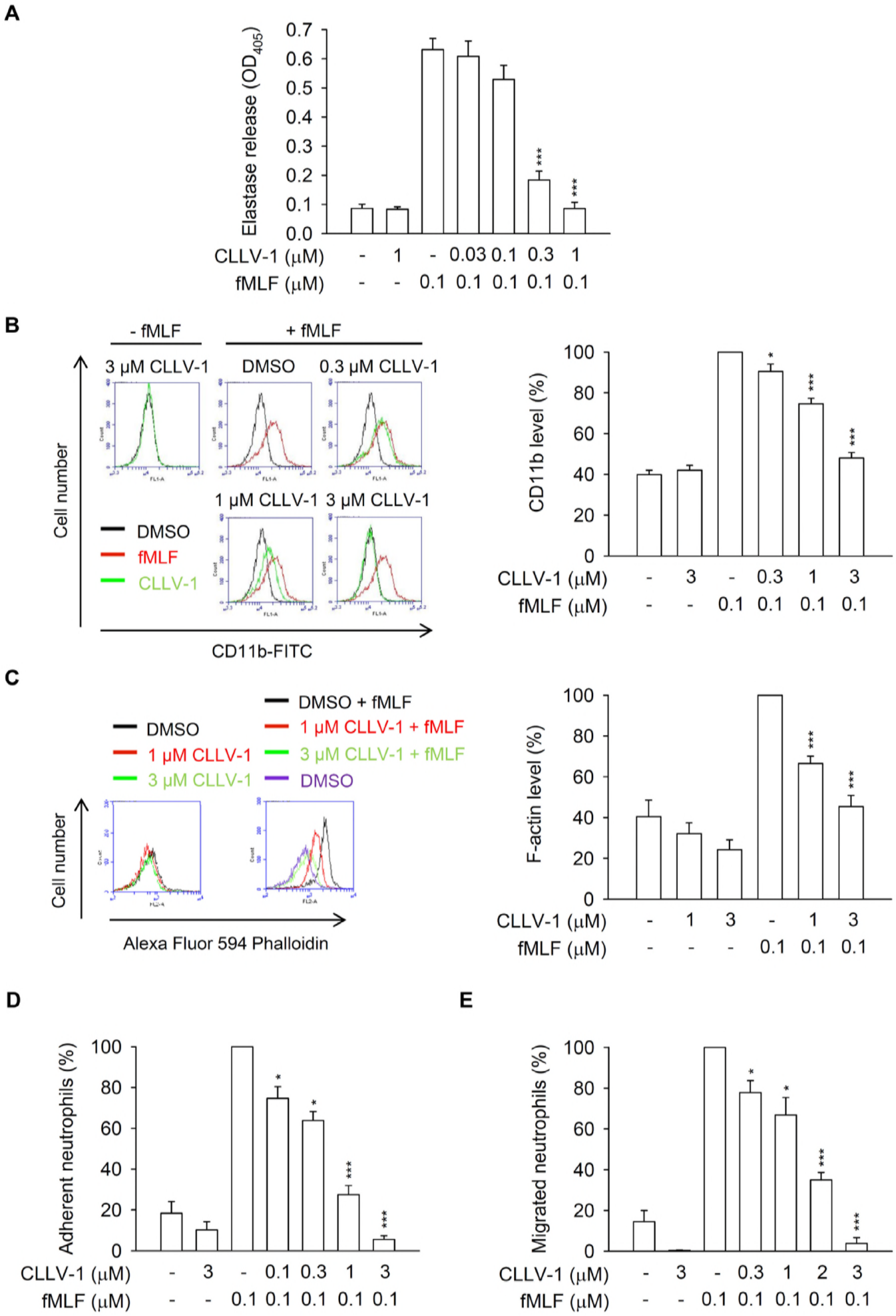

Figure 3

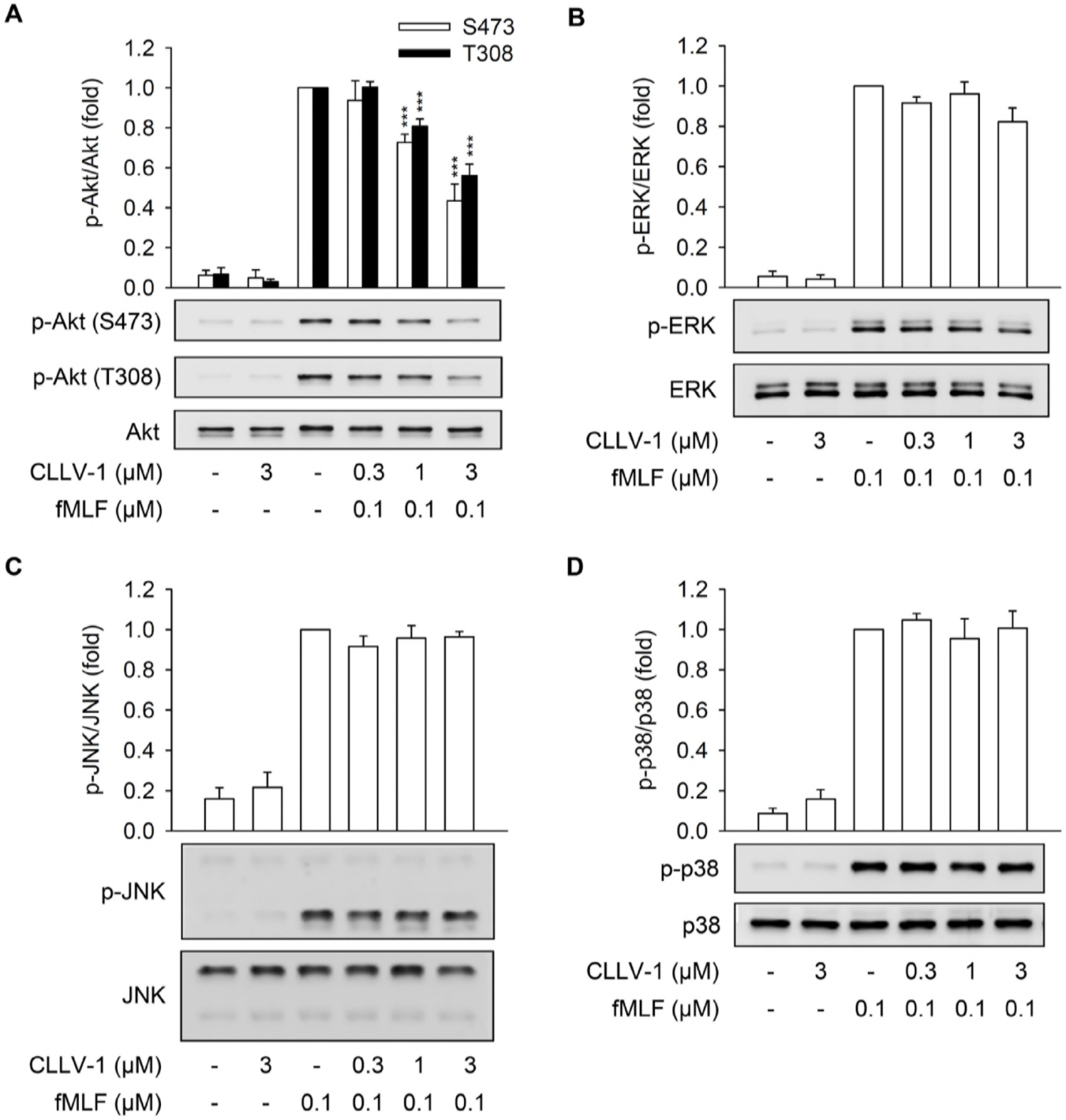

Figure 4

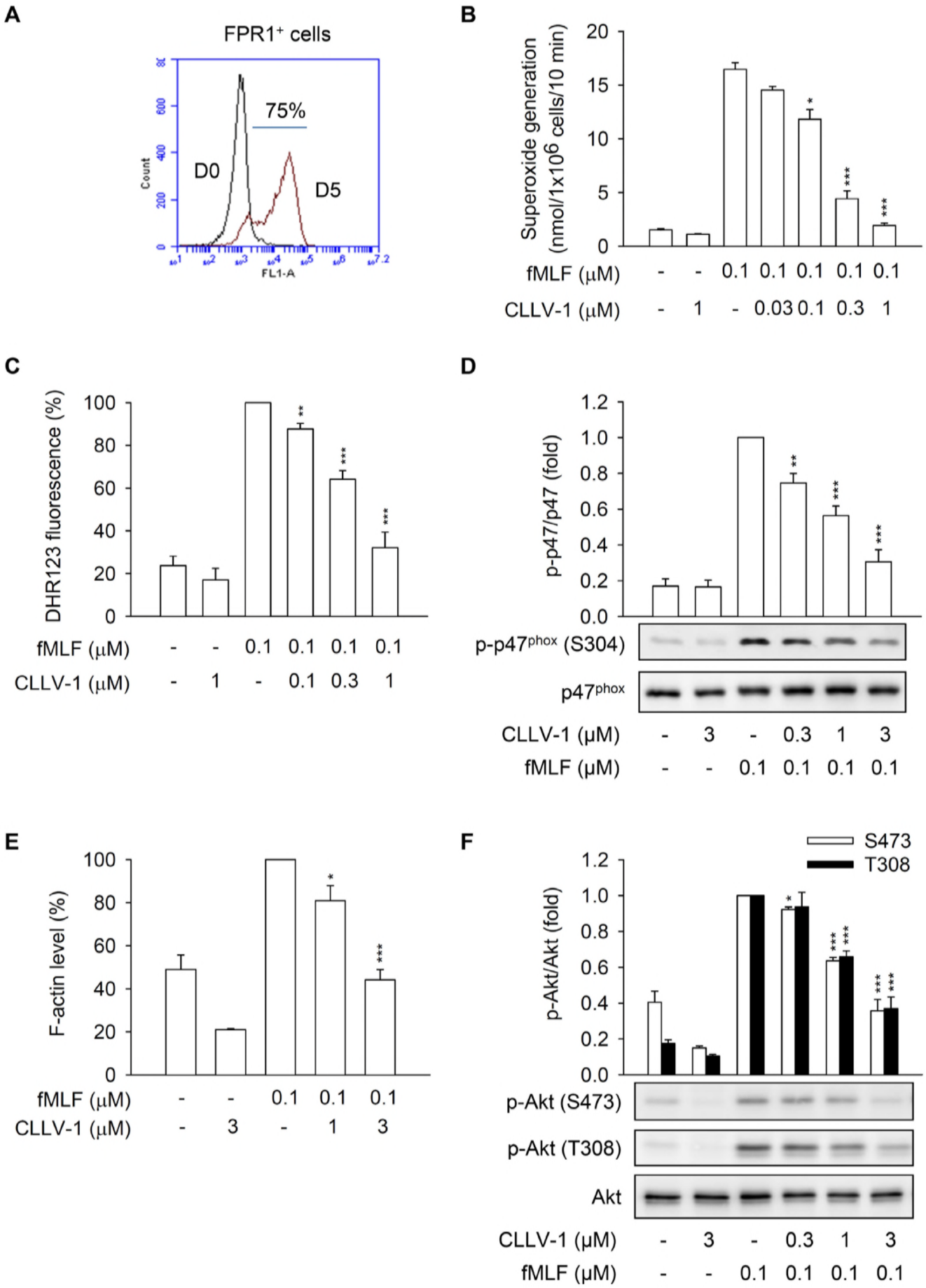

Figure 5

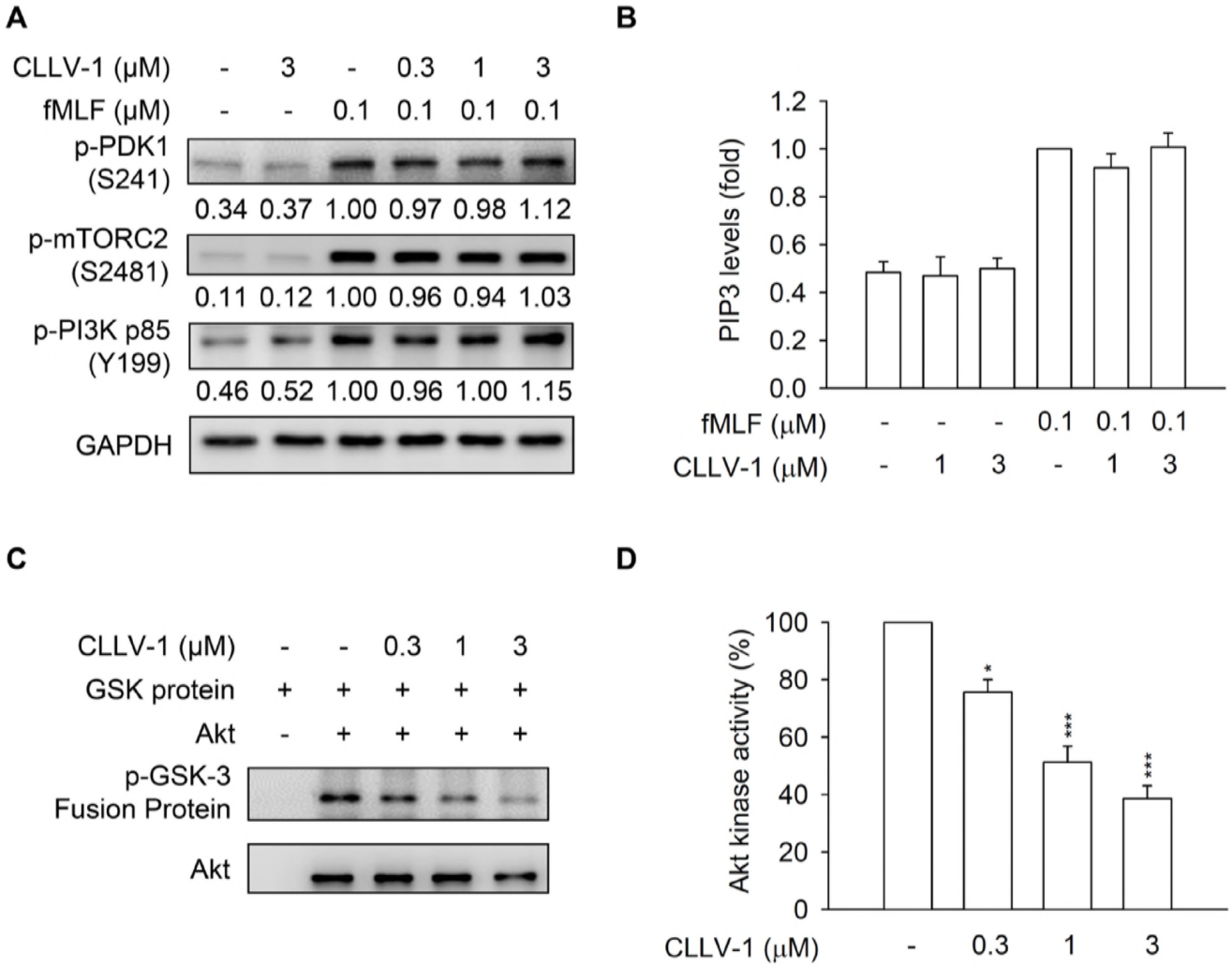

Figure 6

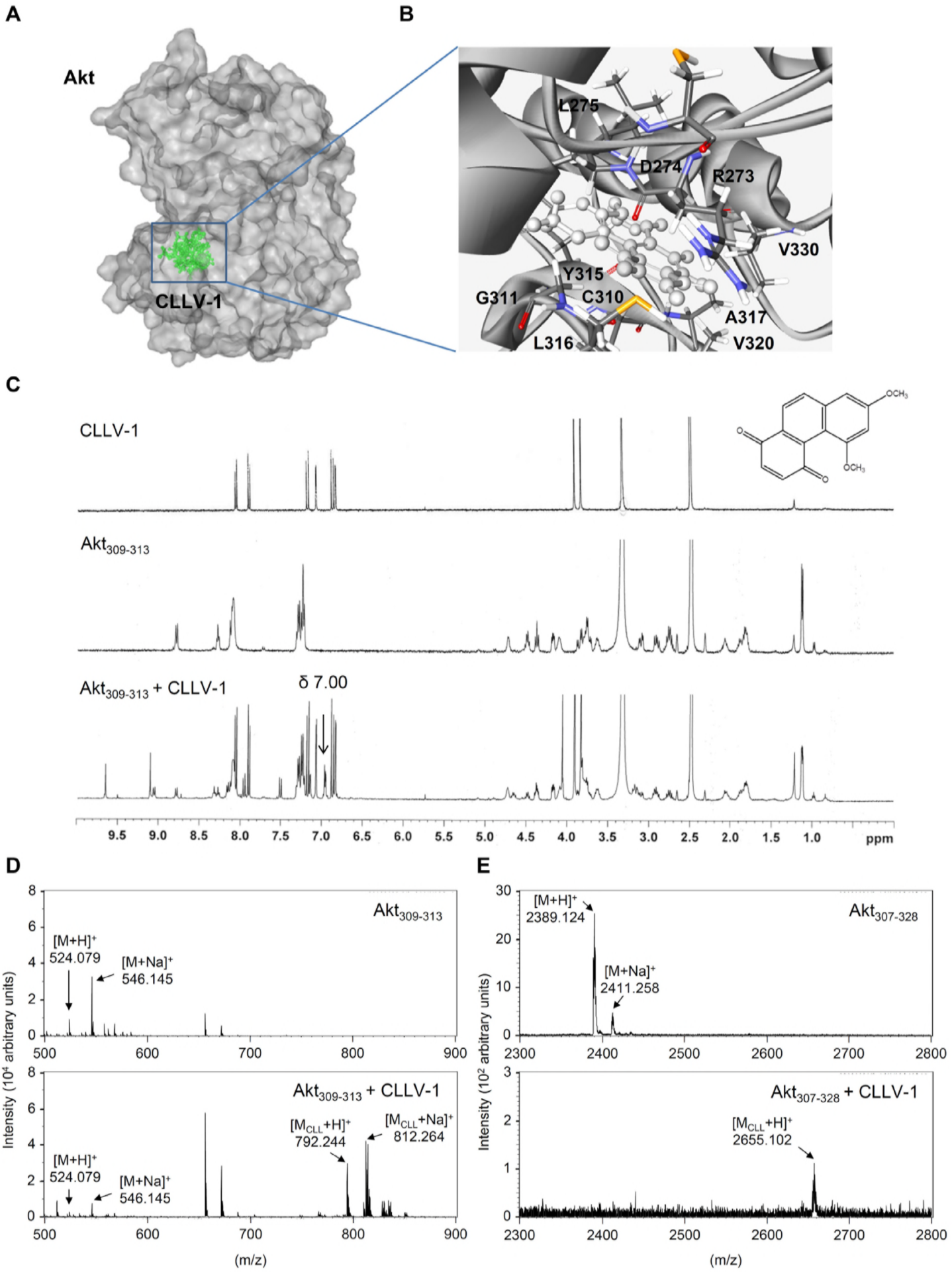

Figure 7

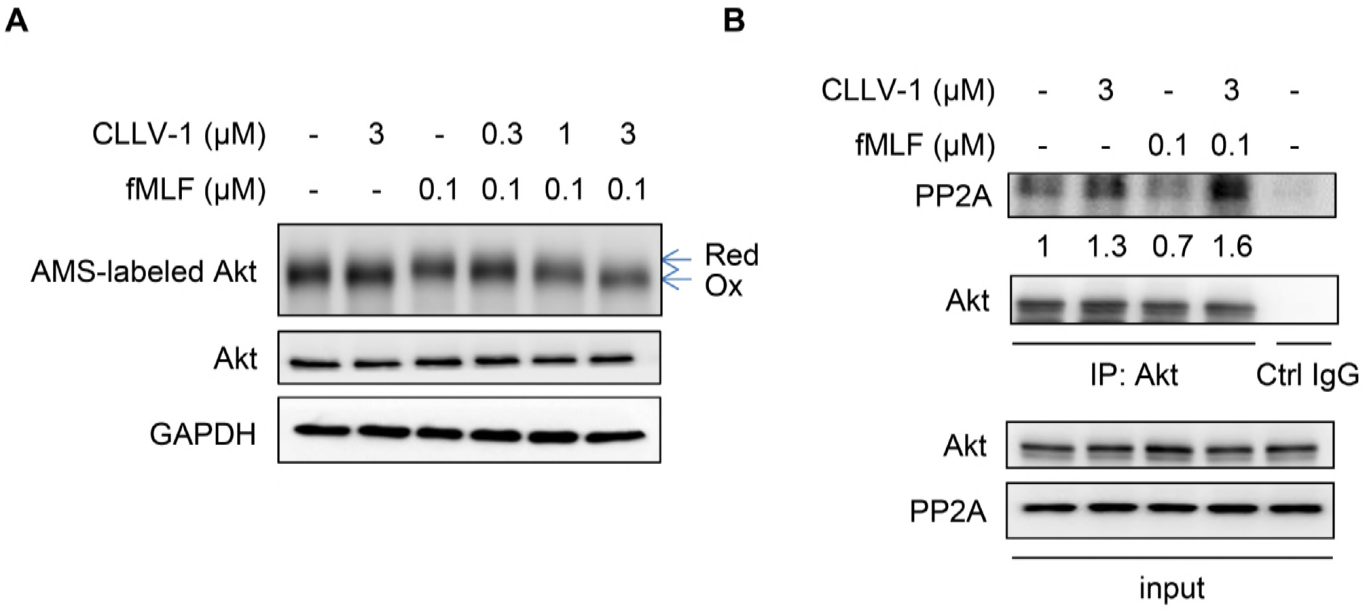
A
CLLV-1 (μM) - 3 - 0.3 1 3
fMLF (μM) - - 0.1 0.1 0.1 0.1
AMS-labeled Akt
Red
Ox
Akt
GAPDH
B
CLLV-1 (μM) - 3 - 3 -
fMLF (μM) - - 0.1 0.1 -
PP2A
1 1.3 0.7 1.6
Akt
IP: Akt
Ctrl IgG
Akt
PP2A
input

Figure 8

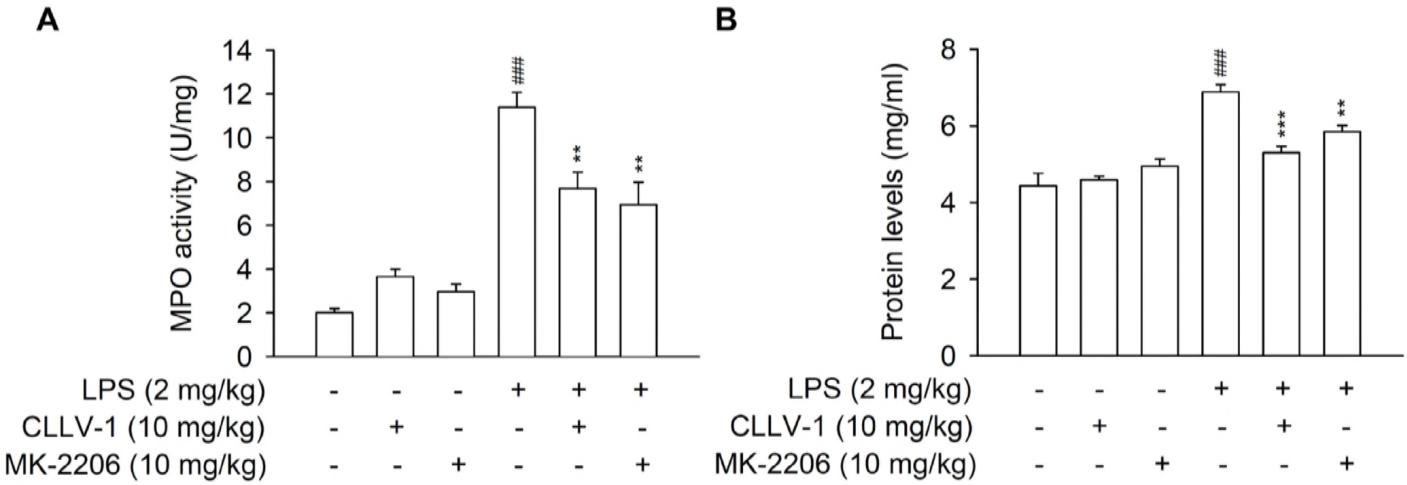

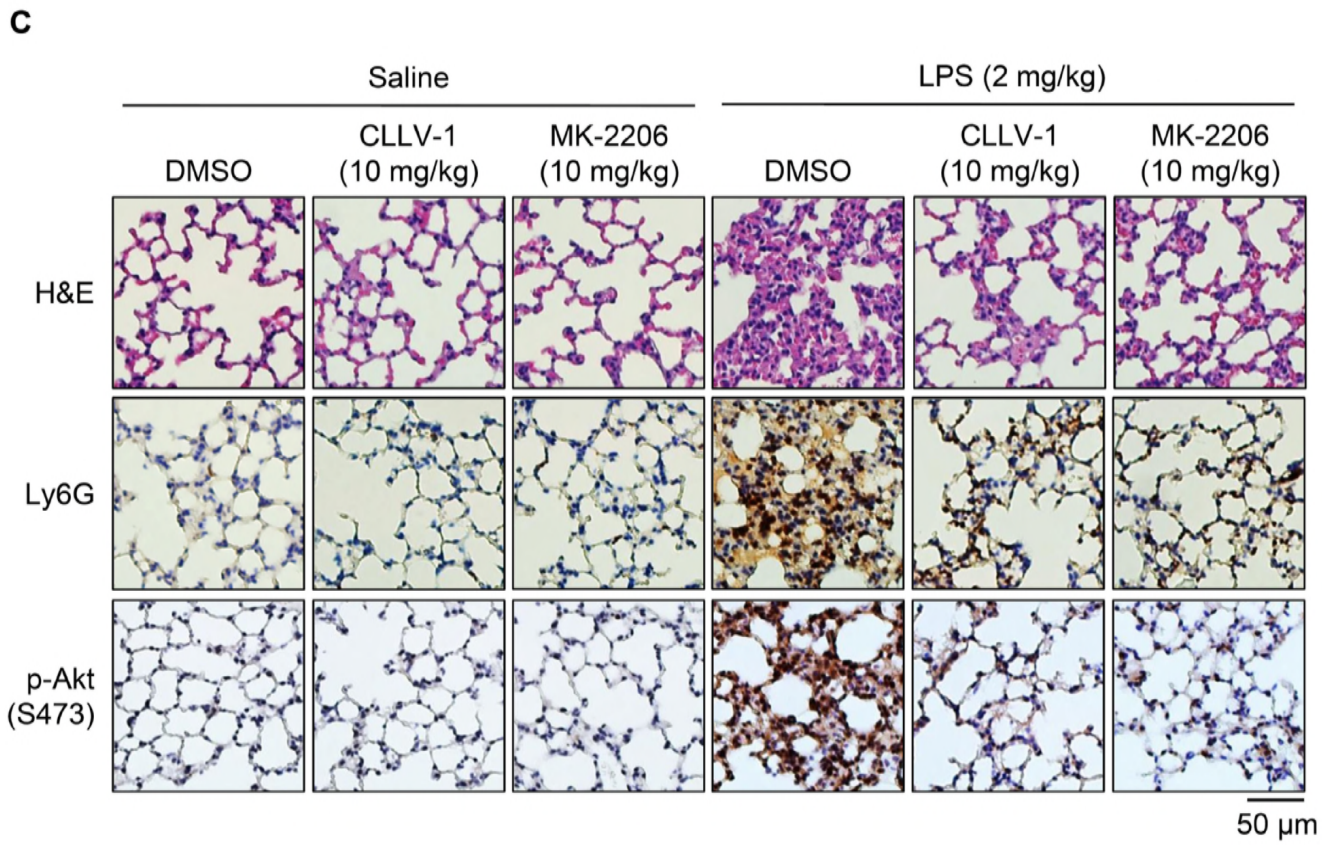

Figure 9

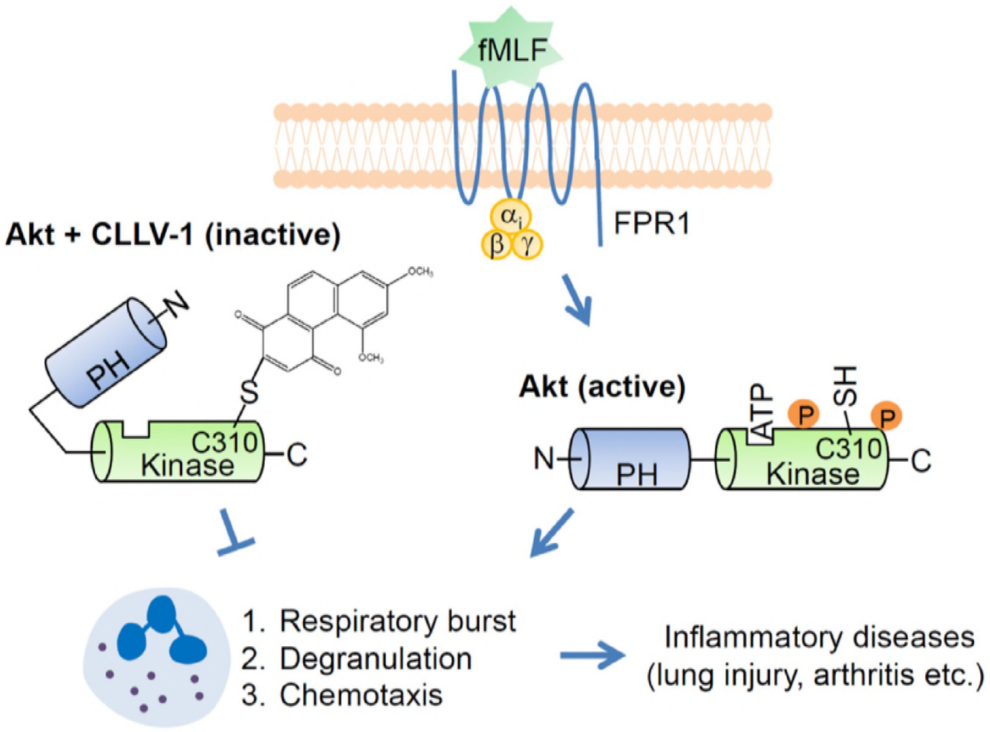

Figure EV1

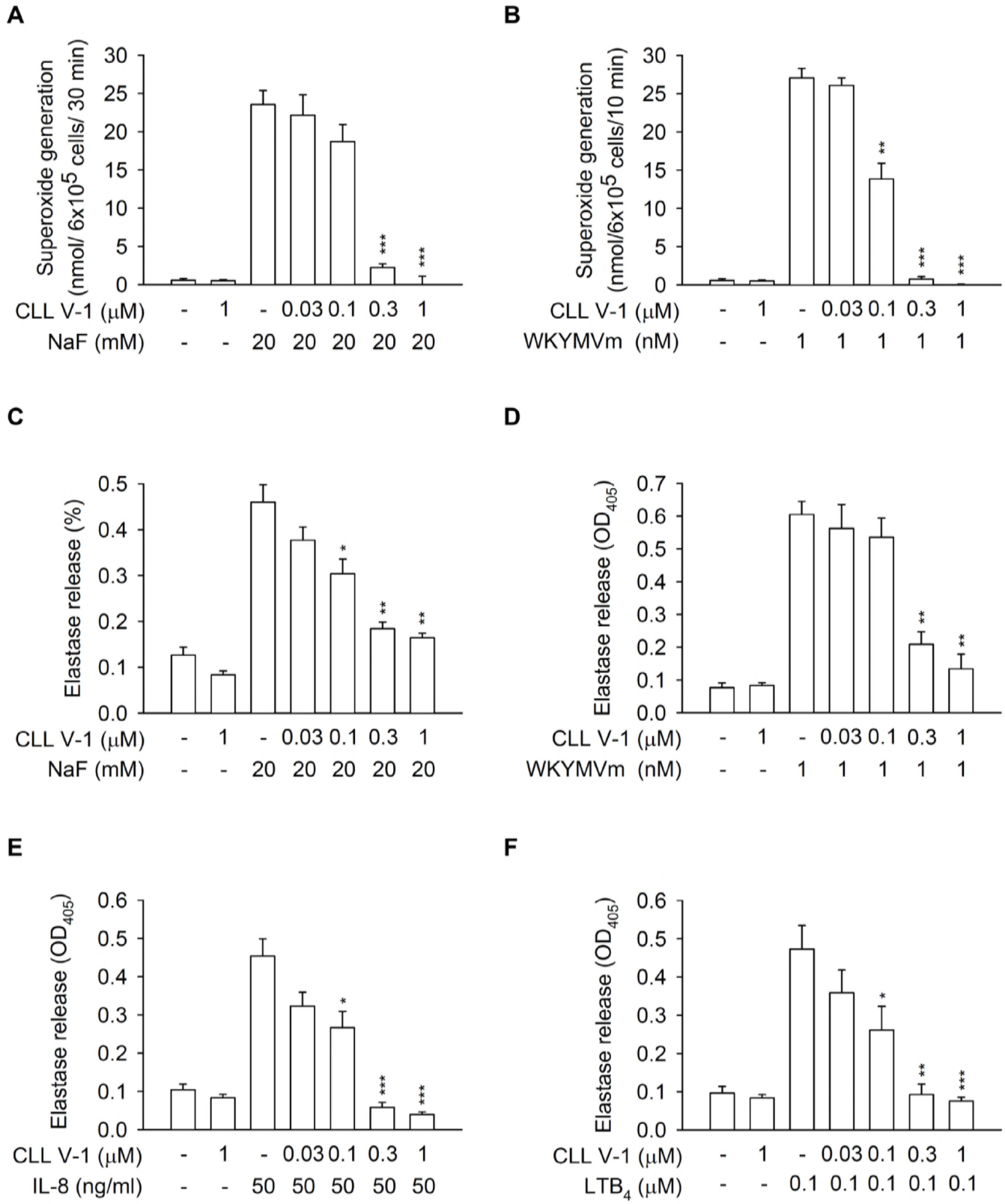

Figure EV2

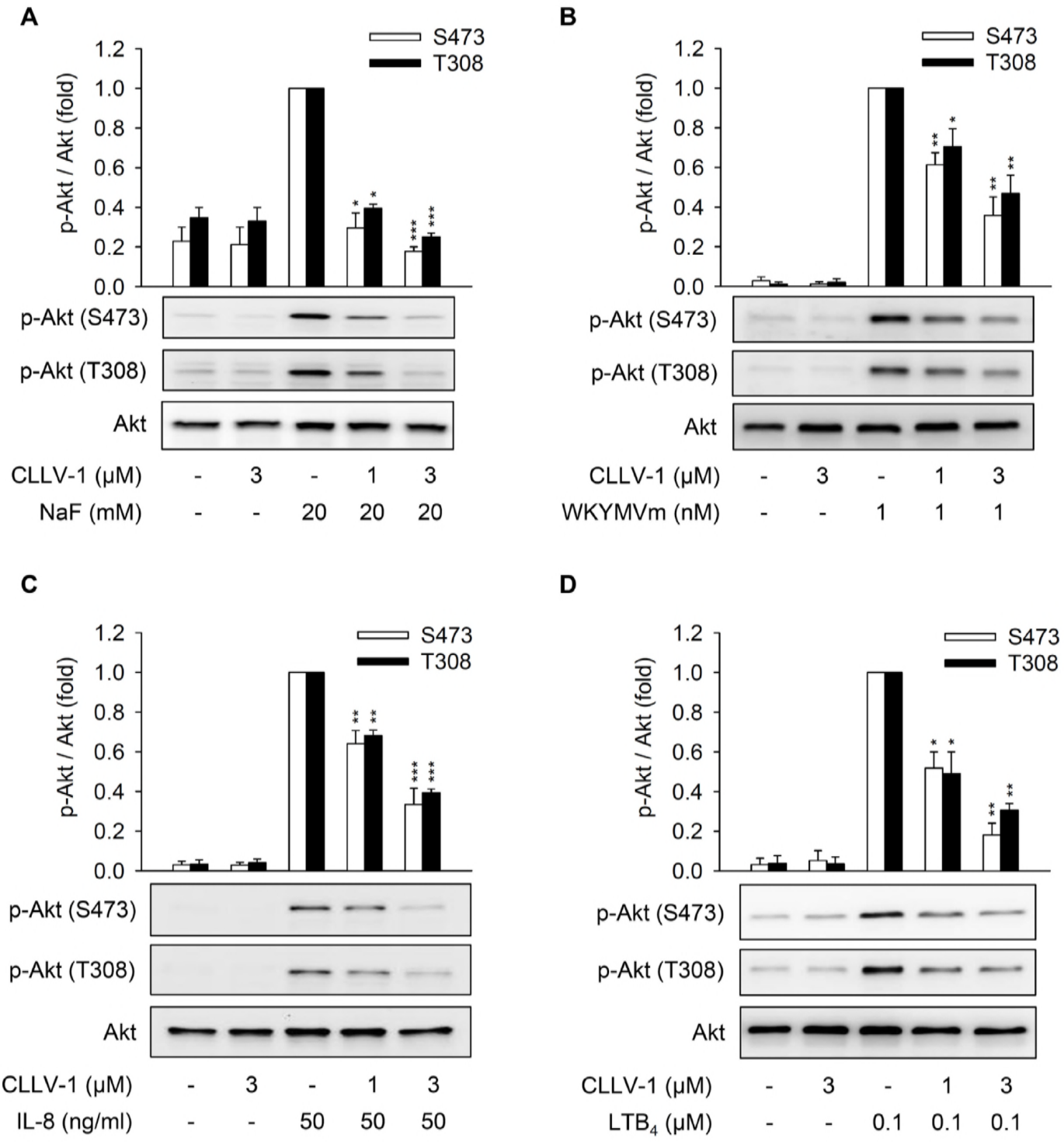

Figure EV3

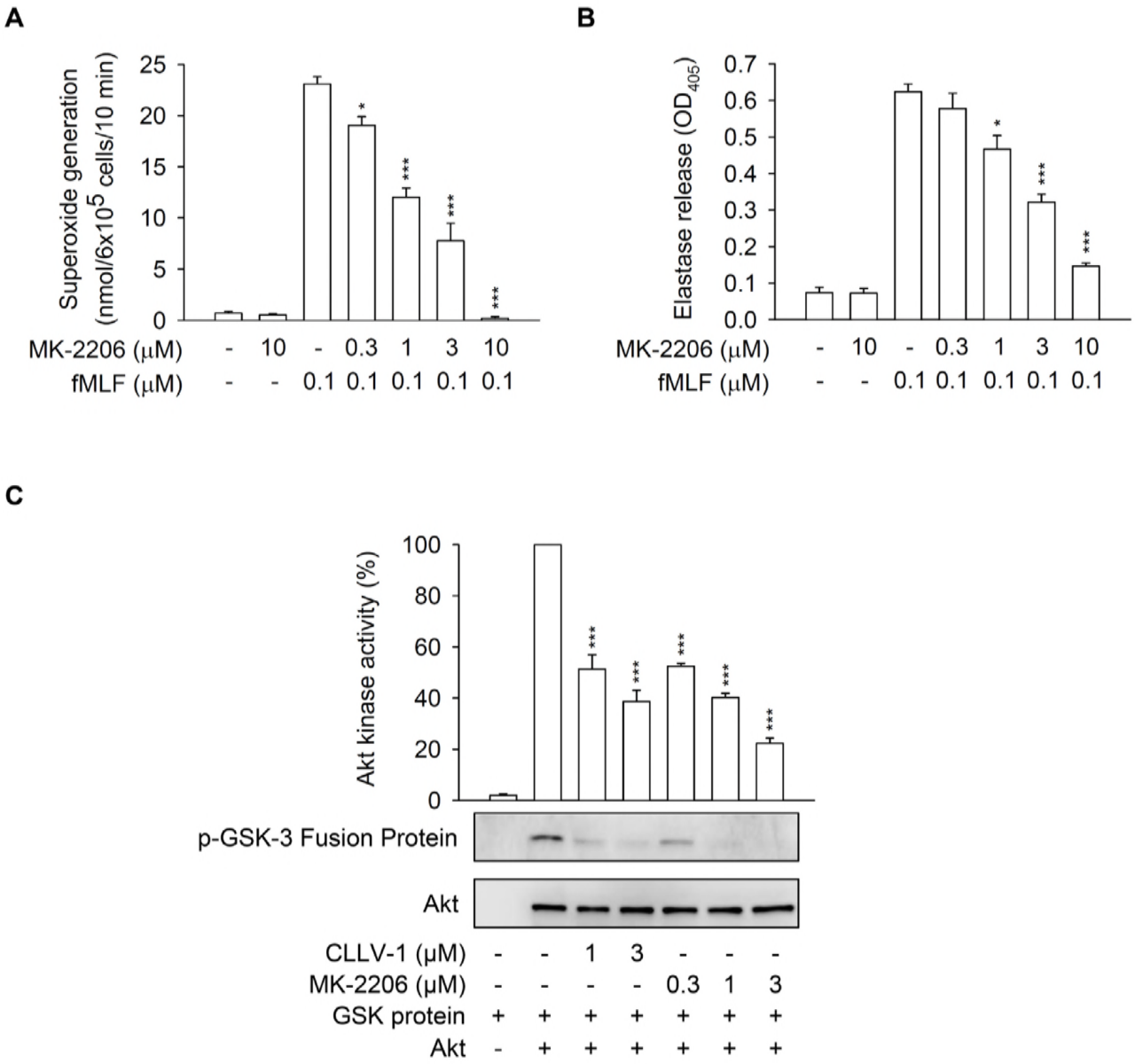
A
Superoxide generation (nmol/6x10^5 cells/10 min)
25
20
15
10
5
0
*
***
***
***
MK-2206 (μM) - 10 - 0.3 1 3 10
fMLF (μM) - - 0.1 0.1 0.1 0.1 0.1
B
Elastase release (OD405)
0.7
0.6
0.5
0.4
0.3
0.2
0.1
0.0
*
***
***
MK-2206 (μM) - 10 - 0.3 1 3 10
fMLF (μM) - - 0.1 0.1 0.1 0.1 0.1
C
Akt kinase activity (%)
100
80
60
40
20
0
***
***
***
***
***
p-GSK-3 Fusion Protein
Akt
CLLV-1 (μM) - - 1 3 - - -
MK-2206 (μM) - - - - 0.3 1 3
GSK protein + + + + + + +
Akt - + + + + + +

Figure EV4

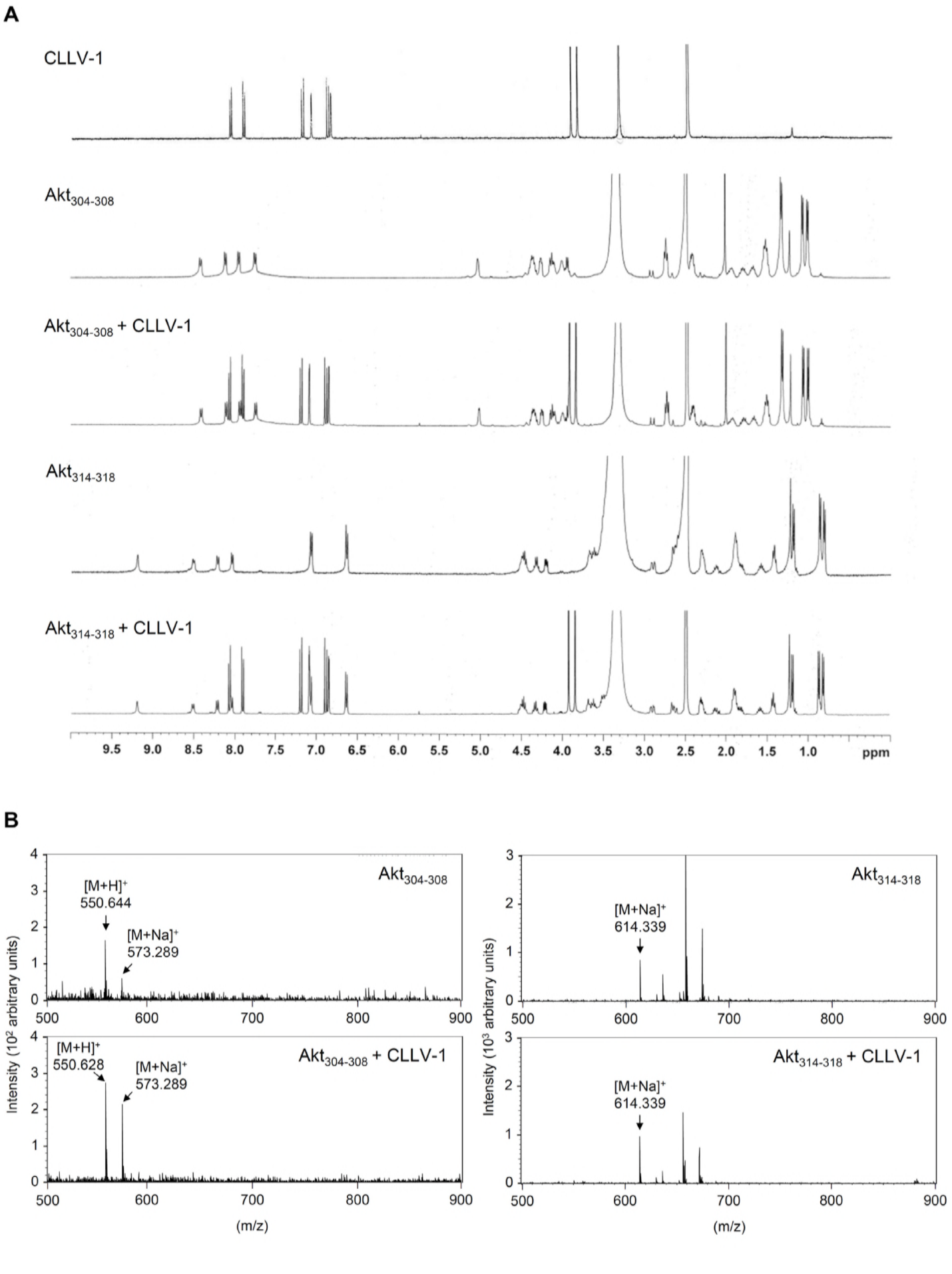

Figure EV5